

Report No. UT-07.11

## **INFLUENCE ON BOND STRENGTH OF PRIOR- TO-CAST CORRODED REINFORCING STEEL**

### **Prepared For:**

Utah Department of Transportation  
Research and Innovation Division

### **Submitted by:**

Brigham Young University  
Department of Civil and Environmental  
Engineering

### **Authored by:**

Fernando S. Fonseca, Ph.D., P.E.  
Brent Wallwork  
Warren K. Lucas, Ph.D., P.E.  
W. Spencer Guthrie, Ph.D.

**October 2006**

**INFLUENCE ON BOND STRENGTH OF PRIOR-TO-CAST CORRODED  
REINFORCING STEEL**

By

Fernando S. Fonseca, Ph.D., P.E.

Brent Wallwork

Warren K. Lucas, Ph.D., P.E.

W. Spencer Guthrie, Ph.D.

A Report submitted to the  
Utah Department of Transportation

October 2006

## **DISCLAIMER**

“The authors alone are responsible for the preparation and accuracy of the information, data, analysis, discussions, recommendations, and conclusions presented herein. The contents do not necessarily reflect the views, opinions, endorsements, or policies of the Utah Department of Transportation or the US Department of Transportation. The Utah Department of Transportation makes no representation or warranty of any kind, and assumes no liability therefore.”

## EXECUTIVE SUMMARY

The reducing in cross sectional area of a reinforcing steel bar (rebar) by corrosion suggests the possibility of decreased bond strength between the rebar and surrounding concrete. The efficacy a common repair method for corroded rebar used in concrete structures is discussed in this report. The method includes removal of concrete damaged by the rebar corrosion, cleaning of the rebar by sandblasting, and placement of a concrete patch material.

The objective of the study was to determine the influence of corrosion-induced rib degradation on maximum load, initial slip load, slip prior to failure, and maximum bond stress. The scope of the study includes two factors: rebar size and degree of corrosion. Three rebar sizes were considered: #5, #8, and #11. Eight levels of corrosion were considered: 0.00%, 0.25%, 1.00%, 2.00%, 5.00%, 7.50%, and 10.0%. A full-factorial treatment structure was used, with three replicates per treatment, for a test matrix of 72 specimens. The experimental unit was a cantilever beam specimen embedded with rebar corroded prior to casting. Pull-out tests were conducted in which bar slippage and applied load were measured. The data were analyzed using several statistical methods including analysis of variance, Tukey's mean separation procedure, and bivariate linear regression. The analyses established that there was insufficient evidence to suggest that corrosion reduces maximum load for all three rebar sizes. Sufficient evidence, however, exists to suggest that corrosion reduces initial slip load for #11 rebars but not for #8 rebars. In addition, sufficient evidence exists to suggest that corrosion increases the slip prior to failure for #5 rebars, but not for #8 or #11 rebars. There was, however, not sufficient evidence to suggest that corrosion reduces maximum bond stress for all three rebar sizes.

## TABLE OF CONTENTS

Page

EXECUTIVE SUMMARY .....	ii
TABLE OF CONTENTS .....	iii
ACKNOWLEDGMENTS .....	iv
LIST OF TABLES .....	v
LIST OF FIGURES.....	vi
1. INTRODUCTION.....	1
1.1 Problem Statement.....	1
1.2 Objectives.....	2
1.3 Scope .....	2
1.4 Organization of Report .....	2
2. BACKGROUND .....	5
2.1 Bond Mechanics .....	5
2.2 Corrosion Process .....	7
2.3 Corrosion Repair .....	9
2.4 Previous Research .....	11
3. EXPERIMENTAL METHODOLOGY .....	15
3.1 Introduction.....	15
3.2 Experimental Design .....	15
3.2.1 Test Specimen Selection .....	15
3.2.2 Test Matrix.....	17
3.3 Specimen preparation .....	18
3.3.1 Accelerated Corrosion .....	20
3.3.2 Rebar Cleaning.....	22
3.3.3 Casting .....	23
3.4 Testing.....	18
3.4.1 Testing Apparatus.....	32
3.4.2 Data Acquisition.....	32
3.4.3 Specimen Modification.....	36

4. DISCUSSION OF RESULTS .....	39
4.1 Statistical Considerations .....	39
4.1.1 Statistical Analysis Background.....	43
4.1.2 Experimental Design Mitigation .....	43
4.2 Maximum Load .....	44
4.2.1 Results.....	49
4.2.2 Discussion .....	49
4.3 Initial Slip Load .....	55
4.3.1 Results.....	59
4.3.2 Discussion .....	49
4.4 Slip Prior to Failure .....	60
4.4.1 Results.....	65
4.4.2 Discussion .....	49
4.5 Maximum Bond Stress .....	65
4.5.1 Results.....	69
4.5.2 Discussion .....	49
5. CONCLUSIONS AND RECOMMENDATIONS .....	71
5.1 Summary .....	71
5.2 Conclusions.....	71
5.3 Recommendations .....	72
6. REFERENCES.....	77

## **ACKNOWLEDGEMENTS**

The authors would like to thank the financial support given by the Utah Department of Transportation and the tremendous assistance of David Anderson.

## LIST OF TABLES

Table 3.1 — Mass Loss Data for #5 Rebar Specimens .....	14
Table 3.2 — Mass Loss Data for #8 Rebar Specimens .....	15
Table 3.3 — Mass Loss Data for #11 Rebar Specimens .....	16
Table 4.1 — Maximum Load (lbs.) .....	33
Table 4.2 — Statistical Analysis Results for Maximum Load .....	34
Table 4.3 — Initial Slip Load (lbs.) .....	43
Table 4.4 — Statistical Analysis Results for Initial Slip Load .....	44
Table 4.5 — Slip Prior to Failure (in.) .....	48
Table 4.6 — Statistical Analysis Results for Slip Prior to Failure .....	48
Table 4.7 — Maximum Bond Stress (psi) .....	52
Table 4.8 — Statistical Analysis Results for Maximum Bond Stress.....	53

## LIST OF FIGURES

Figure 2.1 — Internal Forces in a Flexural Member .....	3
Figure 2.2 — Forces on Rebar .....	3
Figure 2.3 — Typical Rib Configuration.....	4
Figure 2.4 — Bond Transfer Mechanism.....	4
Figure 2.5 — RC Column with Spalled Concrete .....	5
Figure 2.6 — Suggested Concrete Removal Layouts .....	7
Figure 2.7 — Stages of Corrosion Repair .....	7
Figure 3.1 — Test Specimen Configurations.....	9
Figure 3.2 — Cantilever Bond Test .....	10
Figure 3.3 — Accelerated Corrosion Apparatus.....	12
Figure 3.4 — Metallic Flaking and Rust.....	13
Figure 3.5 — Specimens after Sandblasting .....	13
Figure 3.6 — Details for a Typical #5 Test Specimen .....	18
Figure 3.7 — Details for a Typical #8 Test Specimen .....	19
Figure 3.8 — Details for a Typical #11 Test Specimen .....	20
Figure 3.9 — Placement of Rebars in Forms .....	21
Figure 3.10 — Completed Specimens .....	23
Figure 3.11 — Test Apparatus Configuration.....	24
Figure 3.12 — Swivel Head and Lower Bearing Plate .....	24
Figure 3.13 — Complete Test Apparatus and Setup .....	25
Figure 3.14 — Positioning of Free End LVDT .....	26
Figure 3.15 — Positioning of Stringpot .....	26
Figure 3.16 — Positioning of Loaded End LVDTs .....	27
Figure 3.17 — Bond Length Adjustment of #5 Rebar Specimens.....	28
Figure 4.1 — Determination of Maximum Load from Load vs. Slip Diagram (Specimen 8-0.25-3 Shown).....	32
Figure 4.2 — Maximum Load vs. Percent Corrosion for #5 Rebar Specimens.....	35

Figure 4.3 — Maximum Load vs. Percent Corrosion for #8 Rebar Specimens.....	35
Figure 4.4 — Maximum Load vs. Percent Corrosion for #11 Rebar Specimens.....	36
Figure 4.5 — Eight Levels of Corrosion Considered in this Study (#8 Rebars Shown) .....	38
Figure 4.6 — Typical Failure Mode of #8 Rebar Specimens (Specimens 8-0.00-2 and 8-10.0-3 Shown) .....	39
Figure 4.7 — Typical Failure Mode of #11 Rebar Specimens (Specimens 11-0.00-3 and 11-10.0-3 Shown) .....	40
Figure 4.8 — Typical Failure Mode of #5 Rebar Specimens (Specimens 5-0.00-1 and 5-10.0-3 Shown) .....	41
Figure 4.9 — Determination of Initial Slip Load from Load vs. Slip Diagram (Specimen 8-0.25-3 Shown).....	42
Figure 4.10 — Typical #5 Rebar Specimen Load vs. Slip Diagram (Specimen 5-2.00-2 Shown).....	42
Figure 4.11 — Initial Slip Load vs. Percent Corrosion for #8 Rebar Specimens.....	45
Figure 4.12 — Initial Slip Load vs. Percent Corrosion for #11 Rebar Specimens.....	45
Figure 4.13 — Determination of Slip Prior to Failure from Load vs. Slip Diagram (Specimen 8-0.25-3 Shown).....	47
Figure 4.14 — Slip Prior to Failure vs. Percent Corrosion for #5 Rebar Specimens.....	49
Figure 4.15 — Slip Prior to Failure vs. Percent Corrosion for #8 Rebar Specimens.....	50
Figure 4.16 — Slip Prior to Failure vs. Percent Corrosion for #11 Rebar Specimens.....	50
Figure 4.17 — Maximum Bond Stress vs. Percent Corrosion for #5 Rebar Specimens.....	53
Figure 4.18 — Maximum Bond Stress vs. Percent Corrosion for #8 Rebar Specimens.....	54
Figure 4.19 — Maximum Bond Stress vs. Percent Corrosion for #11 Rebar Specimens.....	54

# 1. Introduction

## 1.1 Problem Statement

Rebar corrosion impacts the function of reinforced concrete structures. A common cause of rebar corrosion is the infiltration of chlorides into concrete, resulting in spalling, cracking, and, eventually, loss of bond strength. Maintaining adequate bond strength between concrete and rebar is critical in ensuring the stability of reinforced concrete structures.

One measure used to mitigate the destructive effects of corrosion is to repair locally affected areas. The repair method involves removal of the concrete surrounding the corroded rebar, cleaning of the corroded rebar by sandblasting, evaluation and possible repair of the rebar, and, finally, recasting. Generally, corroded rebar is replaced, or supplementary reinforcement is added, if loss of rebar cross section exceeds 25% for a single bar or 20% for two or more adjacent rebars (Emmons 1994). For lesser corrosion levels, however, there is still significant degradation of rebar ribs. The ribs provide mechanical interlock between the concrete and the rebar which is necessary for achieving adequate bond strength. Therefore, degradation of the ribs may decrease the bond strength between concrete and rebar.

## 1.2 Objectives

The main objective of the project was to evaluate the bond strength of rebars that have been corroded prior to casting. Such a scenario is applicable to the repair situation in which the rebar is corroded and sandblasted prior to recasting. Specifically, the objective was to determine the influence of prior-to-cast rebar corrosion on maximum load, the load at which initial slip occurs, the amount of slip occurring prior to complete bond failure, and on the maximum bond stress.

## 1.3 Scope

The scope of the research was limited to a range pertinent to most construction applications. The previously mentioned bond effects were studied for three sizes of rebars: #5, #8, and #11. Eight target corrosion levels were considered for each rebar size, including 0.00%, 0.25%, 0.50%, 1.00%, 2.00%, 5.00%, 7.50%, and 10.0%. The study was limited to a single concrete strength of 5000 psi.

## **1.4 Organization**

Following this introductory section, section 2 provides information on bond mechanics, the process of corrosion, corrosion repair, and previous research. Section 3 discusses the methodology of the experiment, including information on the design of the experiment, preparation of the specimens, and specimen testing. Section 4 provides a discussion of the test results, including statistical considerations relevant to the research. Finally, section 5 lists the conclusions from the research and potential avenues for additional study.

## 2. Background

### 2.1 Bond Mechanics

Reinforced concrete design is based on the assumption that the concrete and the rebar combines to create a new, composite material. Generally, the concrete is designed to carry the compressive loads while the rebar is designed to carry the tensile loads. Figure 2.1 illustrates both the internal compressive (C) and tensile (T) forces in a flexural member (beam). There must be a bond between the rebar and the concrete if the rebar is to carry the tensile load and maintain equilibrium. Bonding is accomplished along and around the surface of the rebar, generating bond stresses acting in opposition to the tensile load, as shown in Figure 2.2.

Bond stresses are generated through three means: adhesion, friction, and bearing on the rebar ribs. Adhesion and friction are less significant contributors. As the tensile force in the rebar increases, the rebar will elongate and, due to Poisson's ratio, the rebar diameter will decrease. When the rebar diameter decreases, the rebar no longer adheres to the concrete. In addition, the reduced rebar diameter reduces the normal force between the concrete and rebar, thereby reducing the frictional force (MacGregor 1997, 287). Thus bearing on the rebar ribs is the primary generator of bonding stresses.

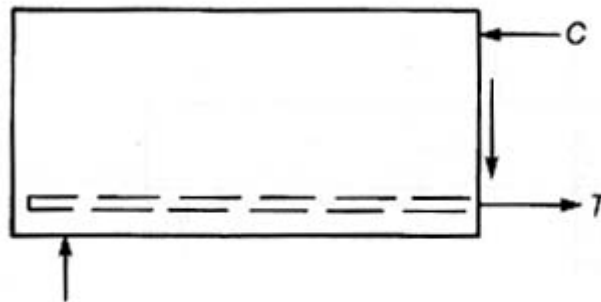


Figure 2.1 Internal Forces in a Flexural Member (MacGregor, 1997)

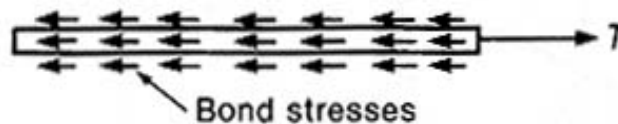
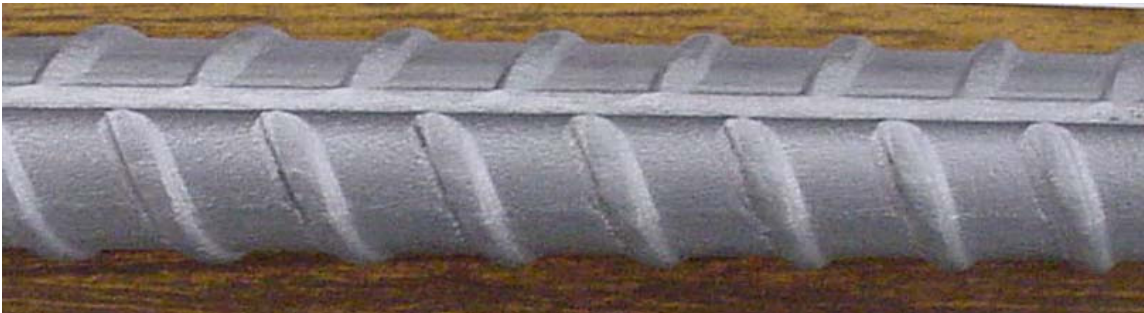
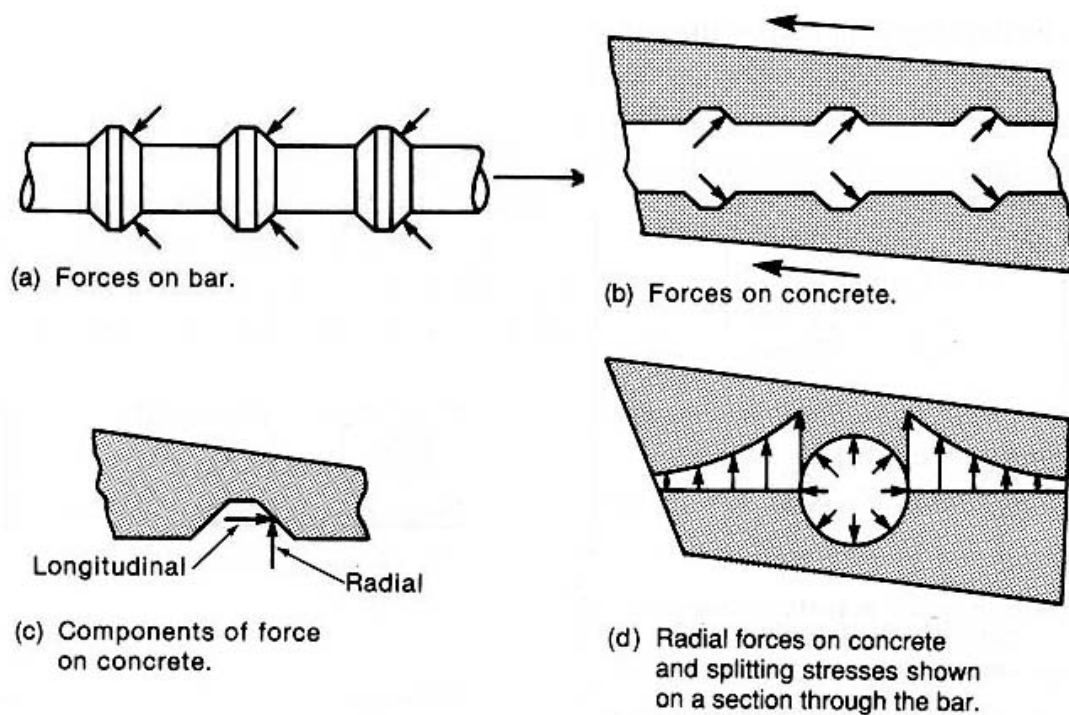


Figure 2.2 Forces on a Rebar (MacGregor, 1997)

Figure 2.3 shows the rib configuration of a typical, non-corroded rebar. Rebars are designed to interlock with concrete. Figure 2.4 shows the interaction between the concrete and rebar. Figure 2.4(a) shows the bearing forces acting on the ribs of the rebar and Figure 2.4(b) shows the equal and opposite forces on the concrete. There are both radial and longitudinal components of the forces on the concrete, as shown in Figure 2.4(c). These forces cause splitting stresses in the concrete, as shown in Figure 2.4(d).



**Figure 2.3 Typical Rib Configuration**



**Figure 2.4 Bond Transfer Mechanism (MacGregor, 1997)**

## 2.2 Corrosion Process

Rebar corrosion is due to an electrochemical process consisting of two half-reactions: oxidation and reduction. Oxidation is the reaction that is destructive to the metal. The location at which oxidation occurs is called the anode. Reduction is the other half-reaction, and involves receiving the electrons released during oxidation. The location at which reduction occurs is called the cathode. During rebar corrosion, the rebar serves as both the anode and cathode. As corrosion proceeds, positively charged ions and electrons are released either adding to the solution or combining with available cations, essentially leaving their metallic state and causing the rebar to deteriorate. Frequently, the oxidation reaction will concentrate on specific points on the rebar, causing pitting (Callister 2000, Integrated 2003).

Moisture and oxygen must be present for corrosion to occur. Both of these may diffuse through the concrete because of its porous consistency. The high alkalinity of new concrete helps prevent corrosion, but when chloride ions are introduced, often through the use of deicing salts, the pH of the concrete decreases, and corrosion can occur (MacGregor 1997).

The rust formed through corrosion has a greater volume than the metal from which it originated. Therefore, the formation of rust causes stresses in the concrete surrounding the rebar and, as formation of rust progresses; the concrete may crack and spall (MacGregor 1997). Figure 2.5 shows a reinforced concrete column with a large section of spalled concrete due to corrosion.



**Figure 2.5 RC Column with Spalled Concrete (Corrosion-Club 2003)**

## 2.3 Corrosion Repair

Costs associated with corrosion repair are significant (Callister 2000). Nonetheless, repair of corroded rebar in reinforced concrete structures often proves to be more economically feasible than rebuilding. A relevant repair method is detailed in this report. The method involves removing the affected concrete, cleaning the corroded rebar, and finally placing new concrete.

Vaysburd et al. (2001) provide a detailed description of the repair method that is summarized here. Consideration must first be given to adequately support the portion of the structure being repaired. Repairs are performed a section at a time, with adequate shoring adjacent to the repair section to ensure that loads are diverted.

Unsound concrete is removed from the deteriorated section. Unsound concrete includes concrete that is cracked due to the expansive action of corrosion, concrete containing corrosion products, and concrete contaminated with chloride. Several means can be employed to do the removing, including diamond-saw cutting, high-pressure water jetting, impacting, and milling. Impacting is most common but may produce microcracking near the surface of the concrete left in place. Additional measures are often required to remove the microcracking to prevent a weak bond plane near the interface between old and new concrete.

Some sound concrete is often removed as well. Rectangular repair geometry is preferred, requiring removal of additional concrete, as shown in Figure 2.6. Cuts shall be made at right angles to the concrete surface, and care shall be taken so as not to damage the rebars.

Concrete surrounding rebars is also removed. The clearance between rebar and surrounding concrete shall be at least 0.75 in. or 0.25 in. larger than the maximum aggregate size used in the repair material. Concrete removal is usually accomplished with a small chipping hammer to help prevent damage to the rebar. Once the concrete is removed, the rebar is inspected to determine if it will need to be repaired or simply cleaned. Generally, if more than 25% of cross section of a single rebar is lost, or 20% for two or more adjacent rebars, cleaning is insufficient. If such is the condition, supplemental rebar is placed alongside the affected length, or the corroded rebar is replaced completely (Emmons 1994).

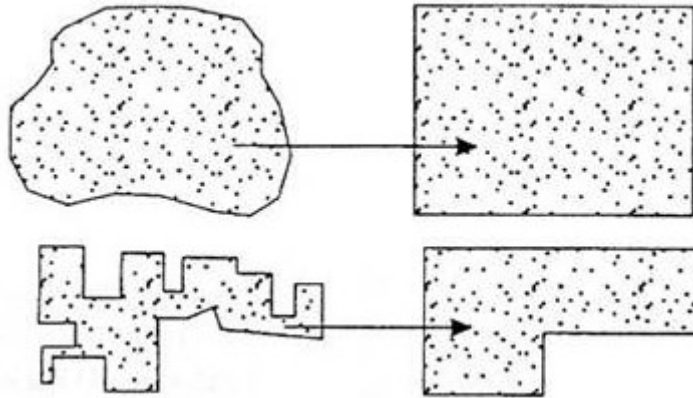


**Figure 2.6 Suggested Concrete Removal Layouts (Vaysburd et al. 2001)**

Sandblasting is the most common cleaning method used to clean corroded rebars. Shotblasting and water jetting are two other available methods. The intent of the cleaning is to remove all remaining corrosion products from the rebar so it will be able to bond to the new concrete. Once the rebar is clean the new concrete is placed and cured. The shoring is then removed and the repaired section resumes its intended use. Figure 2.7 illustrates the stages of the typical repair process.

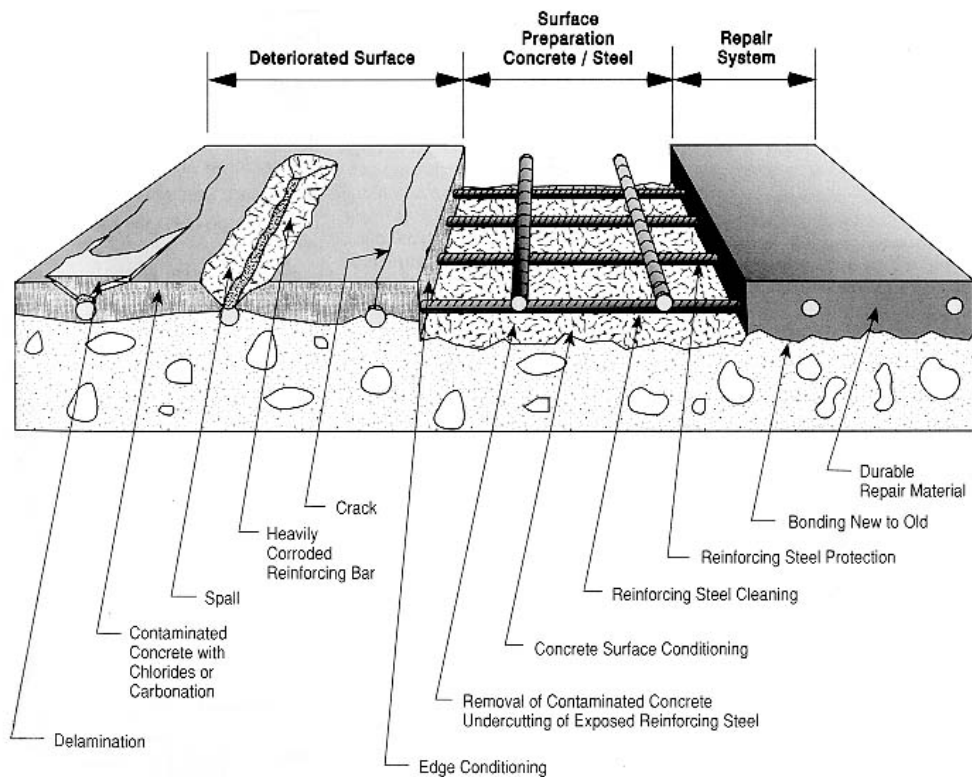


**Figure 2.7 Stages of Corrosion Repair (Emmons 1994)**

## 2.4 Previous Research

Research has been conducted to determine the effect of rust on rebars such as when rebars are stored prior to placement. Morgan (1998) provides a review and summary on the effects of rust formed during storage. The consensus is that loss of bar cross-section is insignificant; strength properties do not change; bond strength increases by the presence of residual rust; and rust may inhibit corrosion in good concrete. Thus the presence of rust is inconsequential.

Research has also been conducted to determine the effects on bond in in-situ corroded rebars. The consensus is that in-situ corrosion severely affects bond strength. Amleh and Mirza (1999) observed that bond strength decreases rapidly with increase in corrosion level. The increased volume of corrosion products formed during the corrosion process generates tensile stresses in the surrounding concrete causing longitudinal cracking which decreases adhesion between concrete and rebar. Al-Sulaimani et al. (1990) observed that bond strength increases for increasing corrosion, up to 1% corrosion. Bond strength increase is due to the increased surface roughness. For higher levels of corrosion, however, a significant decrease in bond strength is common. The decrease is due to the deterioration of the interlock between concrete and rebar ribs and the lubricating effect of the flaky corroded metal. Auyeung, Balaguru, and Chung (2000); Fu and Chung (1997); and Mangat and Elgarf (1999) observed similar effects.

Modifications have been made to rebar ribs in an effort to increase bond strength and research has been conducted to quantify the effects on bond of such alterations. Darwin and Graham (1993) determined the effect of rib spacing and height on bond strength. Corrosion does not affect rib spacing but certainly affects rib height. The measuring parameter of the study was the relative rib area, defined as the ratio of projected rib area normal to the bar axis to the product of nominal bar perimeter and center-to-center rib spacing. Several 1-in.-diameter rebar were machined with varying rib height and rib spacing to model different relative rib areas. Rebars were cast in concrete blocks and pull-out tests were conducted to measure bond capacity. The conclusion was that bond capacity decreases with a decrease in the relative rib area which indicates that corrosion will also decrease bond capacity.

### 3. Experimental Methodology

#### 3.1 Introduction

In order to quantify the influence of prior-to-cast rebar corrosion on bond strength, pull-out tests were conducted on prior-to-cast corroded rebars for various levels of corrosion and rebar size. Load and bar slippage were measured for each specimen. Rationale behind the experimental design, details of the specimen preparation, and details of the specimen testing are described in this section.

#### 3.2 Experimental Design

##### 3.2.1 Test Specimen Selection

There have been different methods to measure bond strength between rebar and concrete, but there is not yet one standardized test. One of the simplest tests is the concentric pull-out test, which is shown schematically in Figure 3.1(a). As the rebar is pulled downward, the bearing plate positioned beneath the specimen provides stability. The pull-out test is criticized by many researchers because the test does not accurately model the mechanics of bond behavior in a true structural application. The argument is that the concrete surrounding the rebar in a structural element, such as in a beam, is in tension while the concrete in the concentric pull-out test is in compression (Chapman and Surendra 1987). Mangat and Elgarf (1999) proposed a hinged-beam design, schematically shown in Figure 3.1(b), which is more representative of the behavior of flexural members. Another test configuration (Auyeung, Balaguru, and Chung, 2000) is a modification from a Danish specification, shown schematically in Figure 3.1(c).

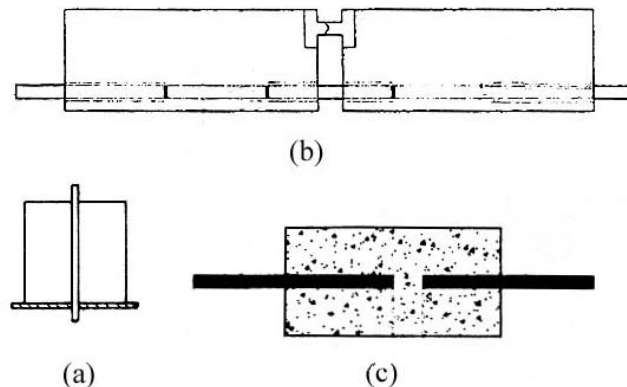


**Figure 3.1 Test Specimen Configurations**

Darwin and Graham (1993) as well as Almusallam et al. (1996) used of a so-called “Cantilever Bond Test”, shown schematically in Figure 3.2. The cantilever bond test simulates bond stresses similar to those experienced by flexural members; bond strains similar to those experienced by the concrete and rebar; and bending moment as well as shear. In addition, the cantilever bond test requires smaller size and less costly specimens. For these reasons, the cantilever bond test was chosen for the study presented in this report. Specific details of the test specimen layout are provided later in this section.

### 3.2.2 Test Matrix

The test matrix was designed considering two factors: rebar size and degree of corrosion. Three rebar sizes were tested: #5, #8, and #11. The corrosion levels were 0.00%, 0.25%, 0.50%, 1.00%, 2.00%, 5.00%, 7.50%, and 10.0%. A full factorial treatment structure was used in the experiment design. That is, all possible combinations of the three bar sizes and the eight corrosion levels were investigated, giving 24 unique treatments. Three replicates were tested for each combination, resulting in 72 test specimens.

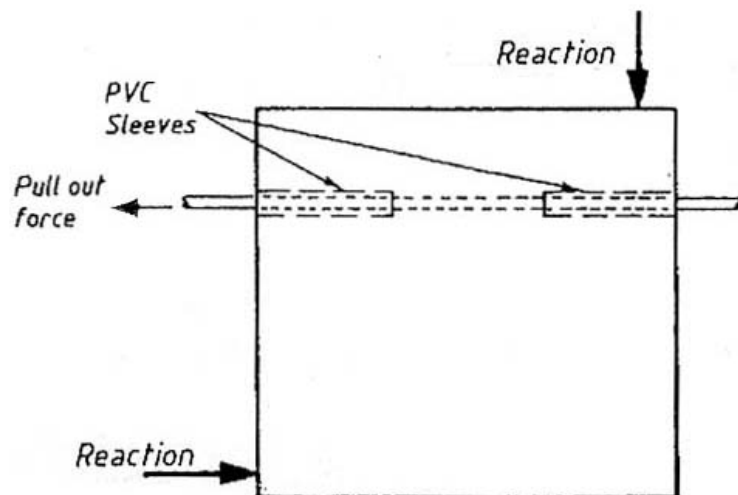


Figure 3.2 Cantilever Bond Test (Almusallam et al. 1996)

### 3.3 Specimen Preparation

#### 3.3.1 Accelerated Corrosion

The rebar for this study was grade 60, new billet steel manufactured by Nucor Steel. Four-foot lengths were used for each specimen.

The method of accelerated corrosion used by Mangat and Elgarf (1999) involving the application of electric current in an electrolyte solution was also used in this study. The method applies Faraday's Law, in which the metal lost due to corrosion is a function of the amount of current applied to the specimen. The application of Faraday's Law is as follows:

$$\Delta w = \frac{AIt}{ZF} \dots\dots\dots \text{(Eq. 3.1)}$$

Where:

$\Delta w$ : Metal lost due to corrosion (oz)

A: Atomic weight of iron (1.975 oz)

I: Corrosion current (amp)

t: Time elapsed (sec)

Z: Valence of the reacting electrode (iron, 2)

F: Faraday's constant (96,500 amp sec)

Four-inch diameter black ABS pipe, capped at one end, was used as container in which to corrode the rebars. Rebars were placed in the container, as well as a four-foot, 0.5-in.-diameter copper pipe. Copper was selected because of its high electrical conductivity. The container was filled with a 3.5% NaCl solution, by weight, used as the electrolyte in the corrosion process. De-ionized water was used for solvent for the NaCl. For ease in handling the level of the solution was such that the top 6 in. of the rebars were not submersed. A Hewlett-Packard 6264B DC Power Supply, with variable amperage, was used as the source of electric current. The positive terminal was connected to the rebars, which served as the anode, while the negative terminal was connected to the copper pipe, which served as the cathode. Figure 3.3 shows the setup.

Rebar corrosion became apparent as the electrolyte solution became dark with metallic by-products. As corrosion levels increased, the solution was replaced multiple times as it became saturated in a matter of hours. The duration and amperage applied to each specimen was determined using Eq. 3.1.



**Figure 3.3 Accelerated Corrosion Apparatus**

At the completion a corrosion cycle, the rebars were removed from the solution, rinsed, and scrubbed with a hand towel. An electronic scale was used to determine the mass loss of each specimen. Percent corrosion was determined from mass loss as a percent of the initial bar mass. The mass loss for each bar was kept to within 10% error of desired mass loss.

### **3.3.2 Reinforcement Cleaning**

Metallic flaking and rust were observed on rebars several weeks after they were corroded and hand-cleaned. Figure 3.4 shows a typical example of the phenomenon. In order to fully clean the bars, sandblasting with a Model AC-2448 Clemco Dry Blast Cleaning Cabinet was utilized. Glass oxide impact beads were used as the abrasive medium. Following sandblasting specimens had a shiny, metallic luster. The shine faded over time as the specimens surface began to oxidize again, but no more flaking or rust was observed. Figure 3.5 shows typical examples of bar appearance immediately following sandblasting.



**Figure 3.4 Metallic Flaking and Rust**

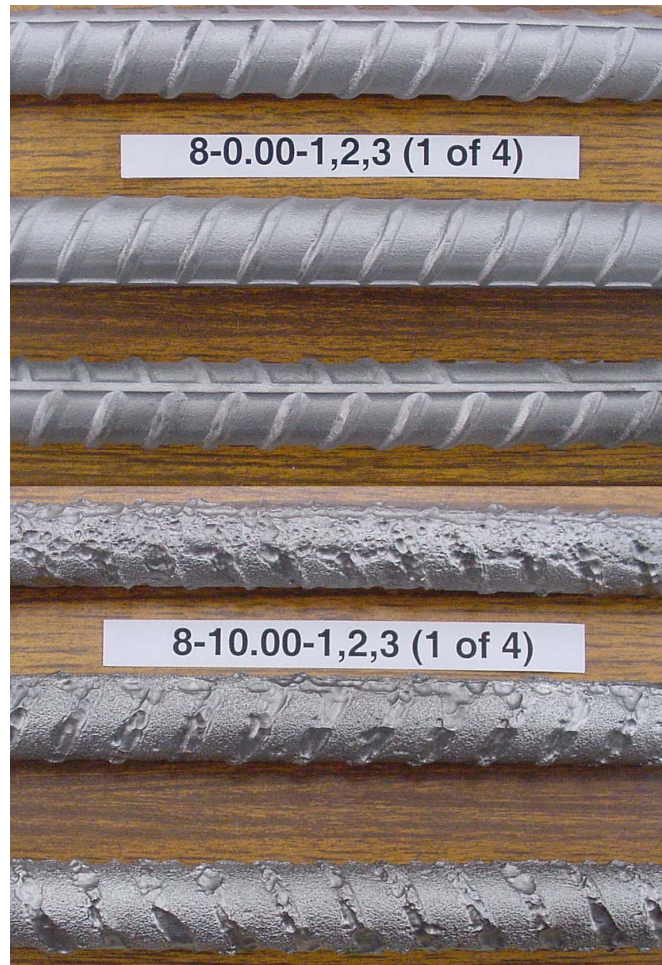


**Figure 3.5 Specimens after Sandblasting**

Tables 3.1 to 3.3 list the mass loss for each specimen. Due to flaking and subsequent sandblasting, the actual mass loss exceeded the target mass loss. In the “Specimen Name” column the first number designates the bar size, the second

designates the target percent corrosion, and the third designates the replicate number. In columns “Initial Mass of Bar,” “Mass of Bar after Corrosion,” and “Mass of Bar after Sandblasting” values for the four-foot lengths are used while in the other columns values are adjusted for the fact that only 42 in. were corroded and sandblasted. “Actual Percent Corrosion” was calculated considering mass loss from both corrosion and sandblasting.

**Table 3.1 Mass Loss Data for #5 Rebar Specimens**

Specimen Name	Initial Mass of Bar (oz)	Required Mass Loss (oz)	Mass of Bar after Corrosion (oz)	Initial Mass Loss (oz)	Initial Percent Corrosion	Mass of Bar after Sand Blasting (oz)	Mass Loss Due to Sand Blasting (oz)	Actual Mass Loss (oz)	Actual Percent Corrosion
5-0.00-1	63.980	0.000	63.980	0.000	0.000	63.641	0.339	0.339	0.605
5-0.00-2	64.019	0.000	64.019	0.000	0.000	63.691	0.328	0.328	0.586
5-0.00-3	64.220	0.000	64.220	0.000	0.000	63.885	0.335	0.335	0.596
5-0.25-1	63.867	0.140	63.729	0.138	0.246	63.341	0.388	0.526	0.940
5-0.25-2	63.789	0.140	63.655	0.134	0.240	63.289	0.367	0.501	0.897
5-0.25-3	63.856	0.140	63.712	0.145	0.259	63.338	0.374	0.519	0.928
5-0.50-1	63.860	0.279	63.581	0.279	0.499	63.225	0.356	0.635	1.136
5-0.50-2	63.765	0.279	63.472	0.293	0.525	63.109	0.363	0.656	1.176
5-0.50-3	63.885	0.279	63.595	0.289	0.517	63.229	0.367	0.656	1.174
5-1.00-1	64.054	0.560	63.490	0.564	1.007	63.112	0.377	0.942	1.680
5-1.00-2	64.022	0.560	63.430	0.593	1.058	63.063	0.367	0.959	1.713
5-1.00-3	63.458	0.555	62.869	0.589	1.061	62.467	0.402	0.991	1.785
5-2.00-1	63.479	1.111	62.386	1.093	1.969	61.895	0.490	1.584	2.851
5-2.00-2	63.673	1.114	62.530	1.143	2.051	62.146	0.384	1.527	2.741
5-2.00-3	63.486	1.111	62.361	1.125	2.026	61.909	0.452	1.577	2.838
5-5.00-1	64.015	2.801	61.073	2.942	5.252	60.706	0.367	3.309	5.907
5-5.00-2	64.019	2.801	61.176	2.843	5.075	60.692	0.483	3.326	5.938
5-5.00-3	64.026	2.801	61.116	2.910	5.195	60.692	0.423	3.333	5.950
5-7.50-1	64.117	4.208	59.863	4.254	7.583	59.310	0.554	4.808	8.570
5-7.50-2	64.220	4.214	59.923	4.296	7.646	59.408	0.515	4.811	8.562
5-7.50-3	64.026	4.202	59.832	4.194	7.486	59.377	0.455	4.649	8.299
5-10.00-1	64.093	5.608	58.146	5.947	10.605	57.793	0.353	6.300	11.234
5-10.00-2	64.086	5.608	58.220	5.866	10.461	57.796	0.423	6.289	11.216
5-10.00-3	63.807	5.583	58.301	5.506	9.862	57.923	0.377	5.884	10.538

**Table 3.2 Mass Loss Data for #8 Rebar Specimens**

Specimen Name	Initial Mass of Bar (oz)	Required Mass Loss (oz)	Mass of Bar after Corrosion (oz)	Initial Mass Loss (oz)	Initial Percent Corrosion	Mass of Bar after Sand Blasting (oz)	Mass Loss Due to Sand Blasting (oz)	Actual Mass Loss (oz)	Actual Percent Corrosion
8-0.00-1	166.415	0.000	166.415	0.000	0.000	165.654	0.762	0.762	0.523
8-0.00-2	165.904	0.000	165.904	0.000	0.000	165.153	0.751	0.751	0.518
8-0.00-3	166.384	0.000	166.384	0.000	0.000	165.668	0.716	0.716	0.492
8-0.25-1	165.343	0.362	164.948	0.395	0.273	164.214	0.734	1.129	0.780
8-0.25-2	164.585	0.360	164.243	0.342	0.238	163.467	0.776	1.118	0.776
8-0.25-3	164.966	0.361	164.592	0.374	0.259	163.883	0.709	1.083	0.750
8-0.50-1	165.096	0.722	164.398	0.698	0.483	163.636	0.762	1.460	1.011
8-0.50-2	164.504	0.720	163.809	0.695	0.483	163.093	0.716	1.411	0.980
8-0.50-3	166.366	0.728	165.643	0.723	0.497	164.853	0.790	1.513	1.040
8-1.00-1	166.447	1.456	164.952	1.496	1.027	164.144	0.808	2.303	1.582
8-1.00-2	166.352	1.456	164.909	1.443	0.991	164.119	0.790	2.233	1.534
8-1.00-3	166.105	1.453	164.567	1.538	1.058	163.749	0.818	2.356	1.621
8-2.00-1	165.784	2.901	162.853	2.931	2.021	162.087	0.765	3.697	2.548
8-2.00-2	163.833	2.867	160.867	2.967	2.069	160.038	0.829	3.795	2.648
8-2.00-3	163.040	2.853	160.211	2.829	1.983	159.325	0.885	3.714	2.604
8-5.00-1	164.059	7.178	156.821	7.238	5.042	155.823	0.998	8.236	5.738
8-5.00-2	164.038	7.177	156.881	7.157	4.986	155.957	0.924	8.081	5.630
8-5.00-3	164.042	7.177	156.609	7.432	5.178	155.505	1.104	8.536	5.947
8-7.50-1	163.347	10.720	152.345	11.002	7.698	151.174	1.171	12.173	8.517
8-7.50-2	164.140	10.772	153.001	11.140	7.756	152.101	0.899	12.039	8.382
8-7.50-3	163.230	10.712	152.080	11.150	7.807	151.308	0.772	11.923	8.348
8-10.00-1	163.149	14.276	148.867	14.282	10.005	147.992	0.875	15.157	10.618
8-10.00-2	162.747	14.240	148.295	14.452	10.148	147.505	0.790	15.242	10.703
8-10.00-3	166.472	14.566	151.040	15.432	10.595	150.338	0.702	16.134	11.076

**Table 3.3 Mass Loss Data for #11 Rebar Specimens**

Specimen Name	Initial Mass of Bar (oz)	Required Mass Loss (oz)	Mass of Bar after Corrosion (oz)	Initial Mass Loss (oz)	Initial Percent Corrosion	Mass of Bar after Sand Blasting (oz)	Mass Loss Due to Sand Blasting (oz)	Actual Mass Loss (oz)	Actual Percent Corrosion
11-0.00-1	327.769	0.000	327.769	0.000	0.000	326.852	0.917	0.917	0.320
11-0.00-2	328.041	0.000	328.041	0.000	0.000	327.081	0.959	0.959	0.334
11-0.00-3	328.192	0.000	328.192	0.000	0.000	327.191	1.002	1.002	0.349
11-0.25-1	327.857	0.717	327.103	0.755	0.263	326.281	0.822	1.577	0.550
11-0.25-2	324.076	0.709	323.307	0.769	0.271	322.422	0.885	1.654	0.583
11-0.25-3	324.270	0.709	323.501	0.769	0.271	322.651	0.850	1.619	0.571
11-0.50-1	328.171	1.436	326.714	1.457	0.507	325.815	0.899	2.356	0.821
11-0.50-2	323.423	1.415	322.023	1.400	0.495	321.088	0.935	2.335	0.825
11-0.50-3	324.898	1.421	323.519	1.379	0.485	322.598	0.921	2.300	0.809
11-1.00-1	328.133	2.871	325.177	2.956	1.030	324.192	0.984	3.940	1.372
11-1.00-2	327.900	2.869	324.891	3.009	1.049	323.974	0.917	3.926	1.368
11-1.00-3	324.806	2.842	321.861	2.945	1.036	320.951	0.910	3.855	1.357
11-2.00-1	327.829	5.737	321.967	5.863	2.044	321.127	0.840	6.702	2.336
11-2.00-2	328.725	5.753	322.803	5.922	2.059	321.974	0.829	6.751	2.347
11-2.00-3	323.289	5.658	317.448	5.841	2.065	316.577	0.871	6.713	2.373
11-5.00-1	323.579	14.157	308.354	15.224	5.377	307.659	0.695	15.919	5.623
11-5.00-2	323.505	14.153	309.194	14.311	5.056	308.256	0.938	15.249	5.387
11-5.00-3	323.734	14.163	308.919	14.815	5.230	307.832	1.086	15.902	5.614
11-7.50-1	324.154	21.273	301.638	22.515	7.938	300.975	0.663	23.179	8.172
11-7.50-2	323.427	3.537	300.591	22.836	8.069	300.100	0.490	23.327	8.243
11-7.50-3	323.917	21.257	302.220	21.697	7.655	300.065	2.155	23.852	8.416
11-10.00-1	324.408	28.386	295.511	28.896	10.180	294.668	0.843	29.739	10.477
11-10.00-2	323.423	28.300	294.548	28.875	10.203	292.774	1.774	30.650	10.830
11-10.00-3	324.072	28.356	294.721	29.351	10.351	293.931	0.790	30.142	10.630

### 3.3.3 Casting

Following sandblasting, rebar specimens were ready for casting. Figures 3.6 to 3.8 show details of the #5, #8, and #11 test specimens, respectively. Several features of the test specimens are noteworthy: the bond length for each rebar is 8.5 in; the PVC pipe surrounding the rebar served as a means of breaking the bond along predetermined locations; the lead length of 4 in. for the bond break was intended to prevent a conical failure of the concrete at the concrete surface during testing; the 8.5-in. bond length was chosen to match the previous research (Darwin and Graham, 1993); the two #6 rebars were included to provide adequate flexural strength; and the four #3 closed stirrups were included to provide adequate shear strength.

Forms were used for casting the specimens. Forms were fabricated from 7/16-in. CDX plywood and reinforced with 2 in. x 4 in. studs. Screws were chosen as fasteners because the forms were intended for casting of multiple specimens. The use of screws enabled the forms to be stripped and if necessary rebuilt with relative ease. Several coats of Minwax Polycrylic Sealant were applied to the interior surface to help prevent the diffusion of moisture from freshly poured concrete into the wood and consequently prevent the forms from warping, further enabling them for multiple casts. A final measure to enable multiple uses was the application a release agent to the interior surface of the forms to ease the stripping after casting.

Test rebars were placed in the forms as shown in Figure 3.9(a). The small holes in the PVC bond breakers were injected with silicone caulking to prevent concrete from penetrating between the rebar and the tubing. Also, rubber bands were wrapped around the rebar at the edge of the bond breakers to provide additional resistance to concrete penetration. Figure 3.9(b) shows the placement of the #6 flexural reinforcement and Figure 3.9(c) shows the placement of the #3 closed shear stirrups.

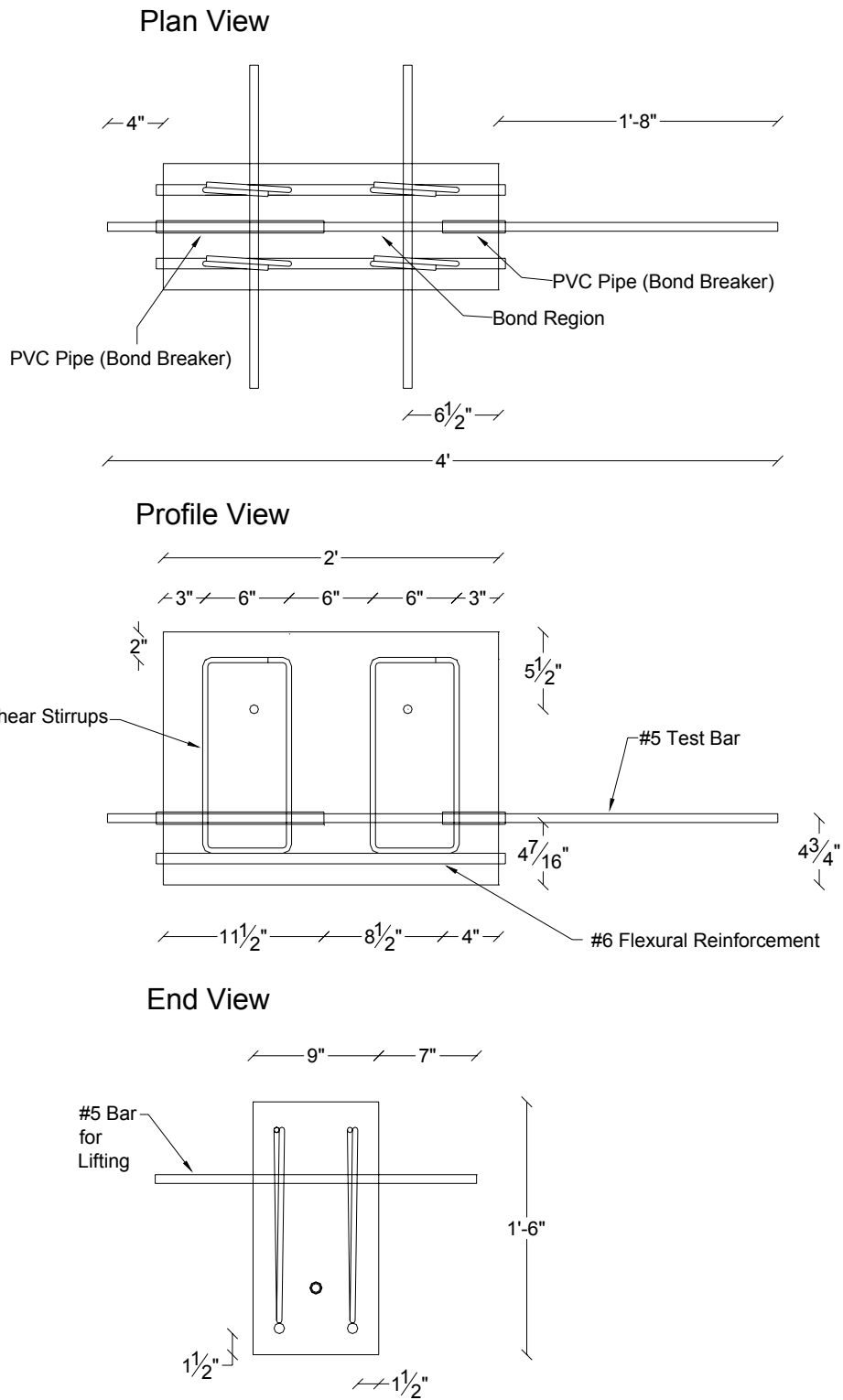
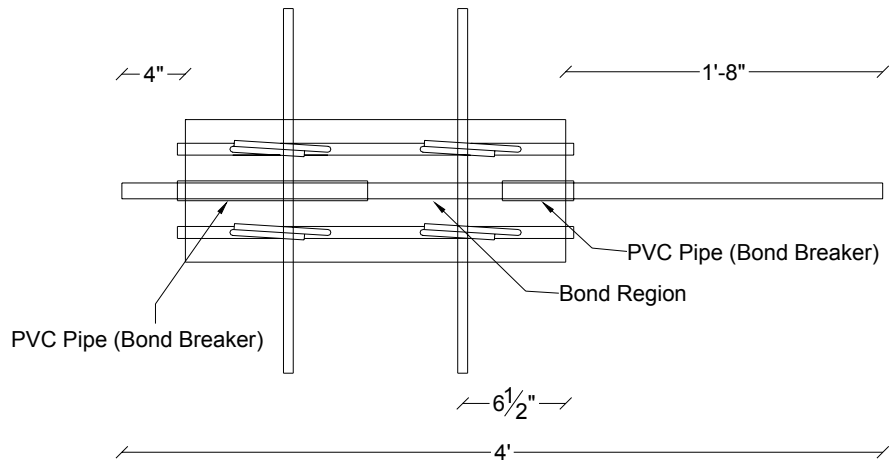
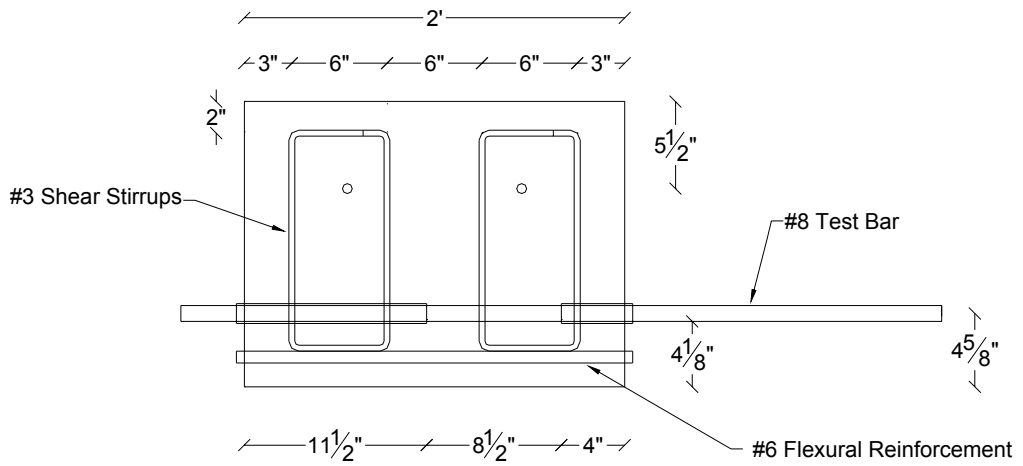


**Figure 3.6 Details for a Typical #5 Test Specimen**

### Plan View



### Profile View



### End View

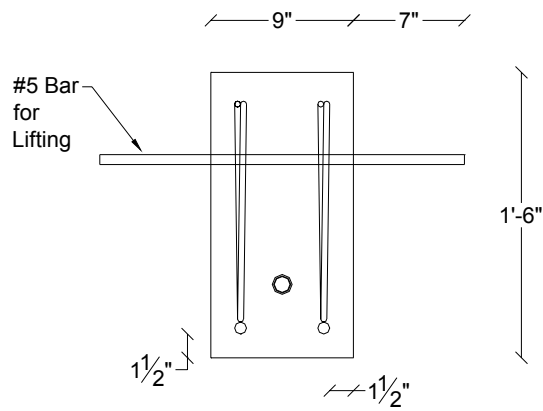


**Figure 3.7 Details for a Typical #8 Test Specimen**

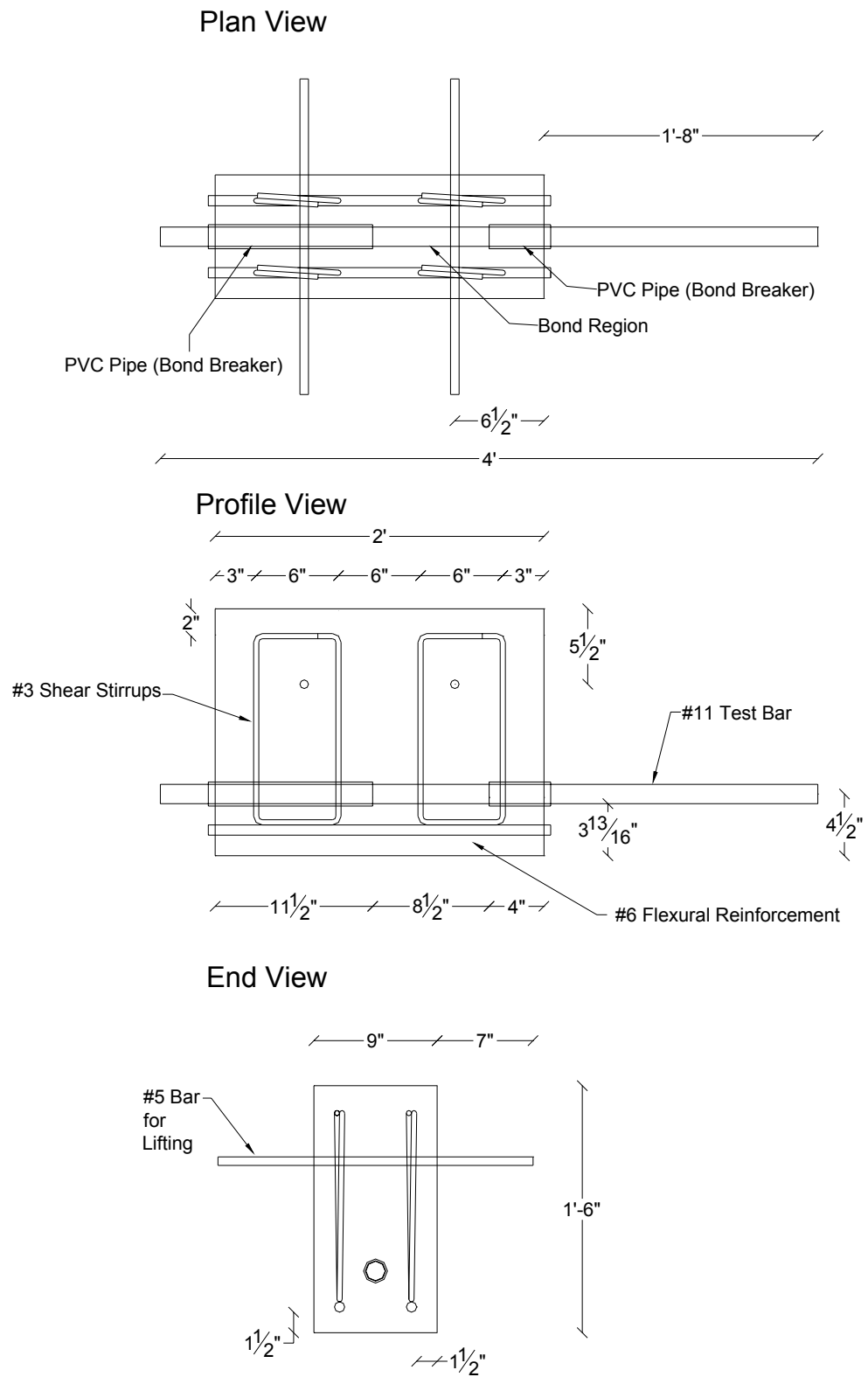


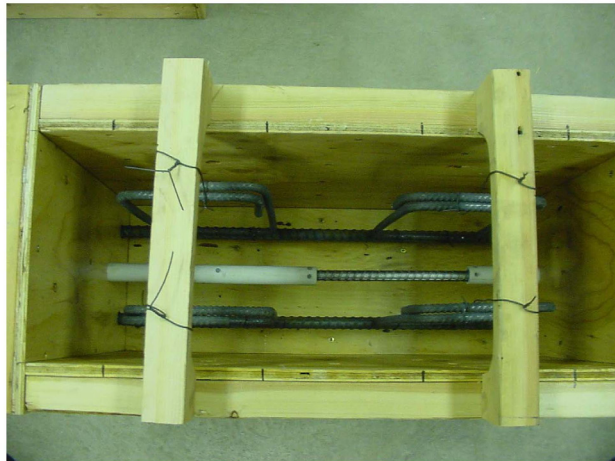
**Figure 3.8 Details for a Typical #11 Test Specimen**



(a)



(b)



(c)

**Figure 3.9 Placement of Reinforcement in Forms**

Test specimens were cast in six separate concrete pours. Twelve specimens were cast per group. Groups were divided by rebar size and corrosion level. For example, the first group consisted of #5 rebar-size specimens, from 0.0% to 1.0% corrosion levels. The second group consisted of #5 rebar-size specimens, from 2.0% to 10.0% corrosion levels. The third group consisted of #8 rebar-size specimens, from 0.0% to 1.0% corrosion levels, and so on. One and a quarter cubic yards of concrete were ordered for each pour. Westroc, Inc. of Pleasant Grove, Utah, was the supplier and delivered the concrete by ready-mix trucks. The compressive strength specified for all six concrete deliveries was 5000 psi. The concrete was placed by chute and shovel and consolidated with a vibrator. Test cylinders were also cast, typically between 14 and 18 cylinders per pour. The cylinders were 4 in. in diameter and 8 in. in length and were prepared according to ASTM C31. Cylinders were cast to determine the average compressive strength of the concrete in each pour as a quality assurance measure. After casting, specimens received a rough finish with a hand trowel, and a tarp was placed on them overnight. Lids were placed on test cylinders overnight, as well.

Forms were stripped the day after casting and specimens were labeled according to rebar size, corrosion level, and replicate number. Each specimen was wrapped in wet burlap and the entire specimen group was covered with a tarp to help maintain the moisture. Specimens were cured for seven days, the burlap being rewetted several times throughout those days. Following curing, specimens were moved and stacked. Figure 3.10 shows several completed specimens.

Test cylinders were also removed from their plastic molds the day after casting. Compressed air was used for the removal. Cylinder were then labeled and placed underneath the tarp together with the specimen group.



**Figure 3.10 Completed Specimens**

### **3.4 Testing**

#### **3.4.1 Testing Apparatus**

Figure 3.11 shows the overall configuration of the testing apparatus. An MTS 100-kip-capacity hydraulic actuator was used for testing. For stability the actuator was mounted to a reaction concrete block that was bolted to the structural laboratory floor. A steel I-beam was also used to support the actuator. A specimen was secured to the actuator via high-strength steel wedge grips. To maintain stability, two bearing points were used. The upper bearing plate was a 5.5 in. x 9 in x 0.5 in steel plate positioned as shown in Figure 3.11 and the lower bearing point was a 2.75 in. x 9 in. x 0.5 in. steel plate with a 10-in.-diameter swivel as shown in Figure 3.12. Figure 3.13 shows the entire testing apparatus.

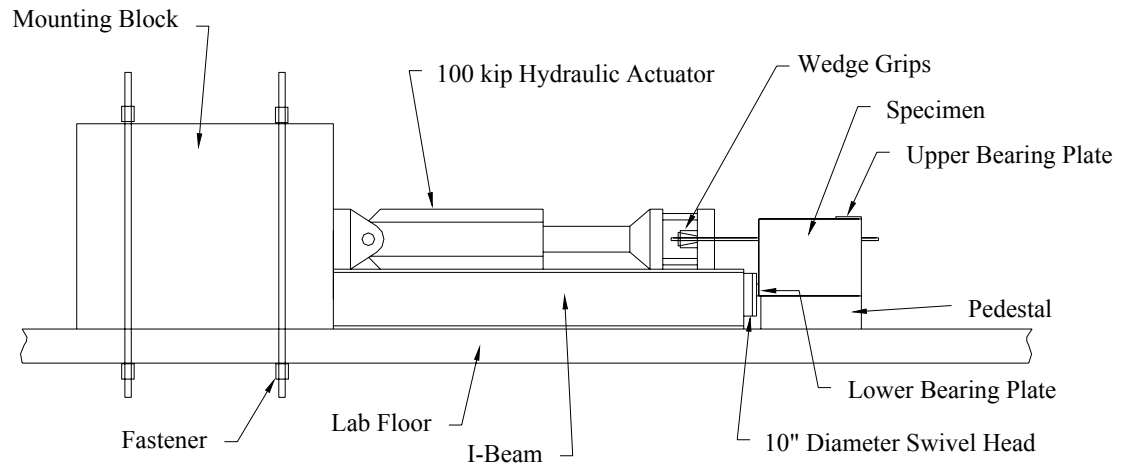


**Figure 3.11 Test Apparatus Configuration**

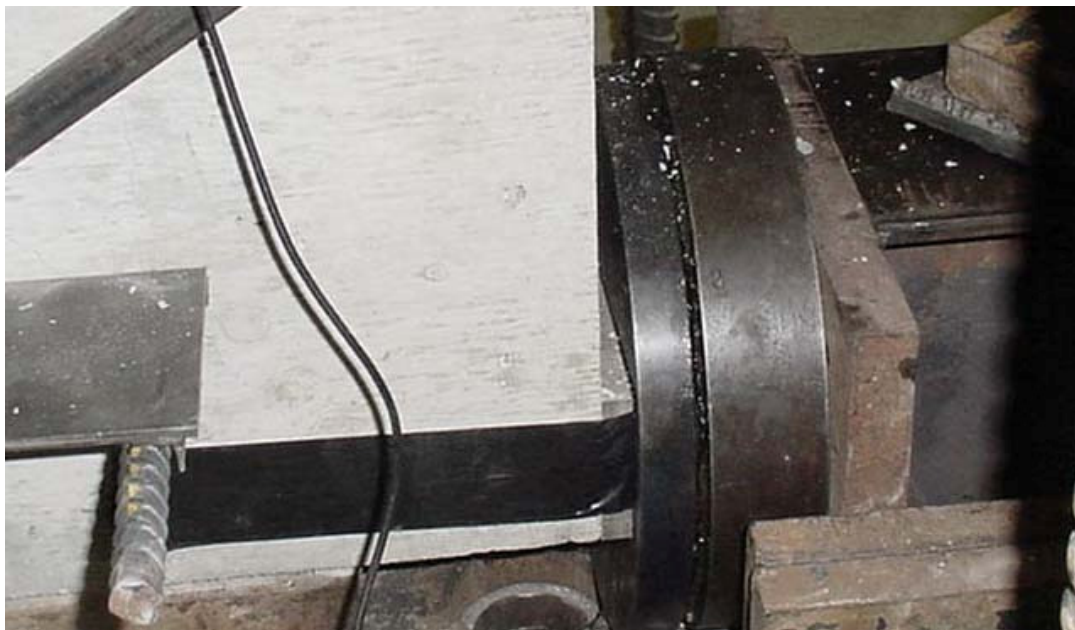


**Figure 3.12 Swivel Head and Lower Bearing Plate**



**Figure 3.13 Complete Test Apparatus and Setup**

### **3.4.2 Data Acquisition**

The actuator load, or pull-out force, increased at a constant rate of 6000 pounds per minute. Load was recorded throughout the duration of each test. Three displacements were measured: the slip at the unloaded or free end of the rebar; the uplift of the specimen; and the slip at the loaded end of the rebar.

One LVDT, secured to the test specimen, was used to measure the slip at the unloaded or free end of the rebar. Figure 3.14 shows the positioning of this LVDT. By securing all LVDTs to the specimen, all measurement were with respect to the specimen.

A stringpot was used to measure the uplift of the specimen and was secured above the upper bearing point. Figure 3.15 shows the positioning of the stringpot. Uplift was monitored to insure that the specimen was rigidly attached to structural floor and testing apparatus. Stringpot data are not included in the discussion of results since uplift data were obtained simply for monitoring purposes.

Two linear variable differential transformers (LVDTs), secured to the test specimens as shown in Figure 3.16, monitored the slip at the loaded end of the rebar. Slip at the loaded end was recorded also for monitoring purposes and, therefore, it is not included in the discussion of results.

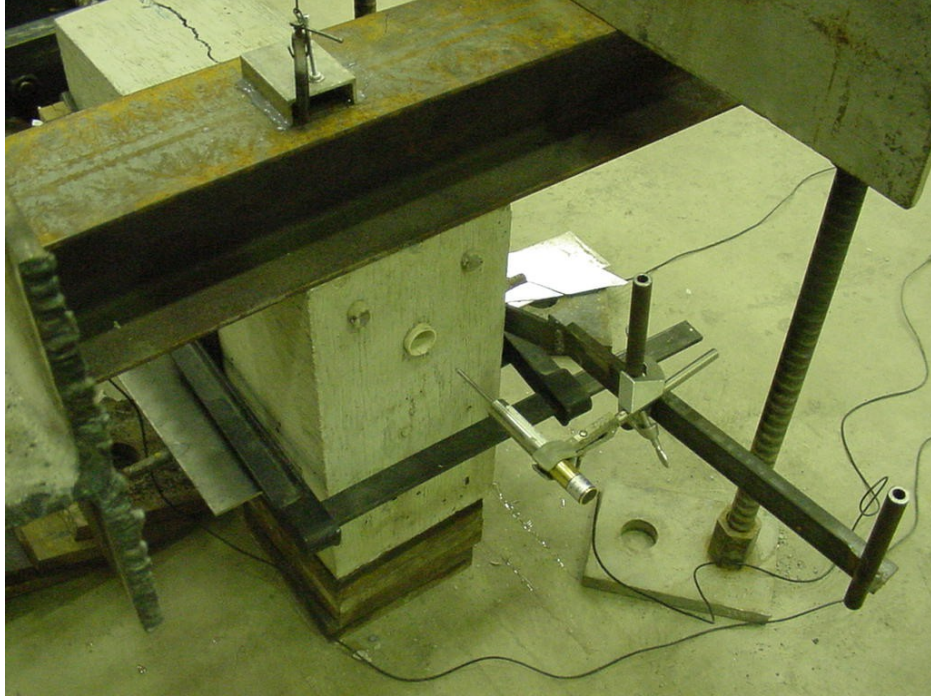


**Figure 3.14 Positioning of Free End LVDT**



**Figure 3.15 Positioning of Stringpot**

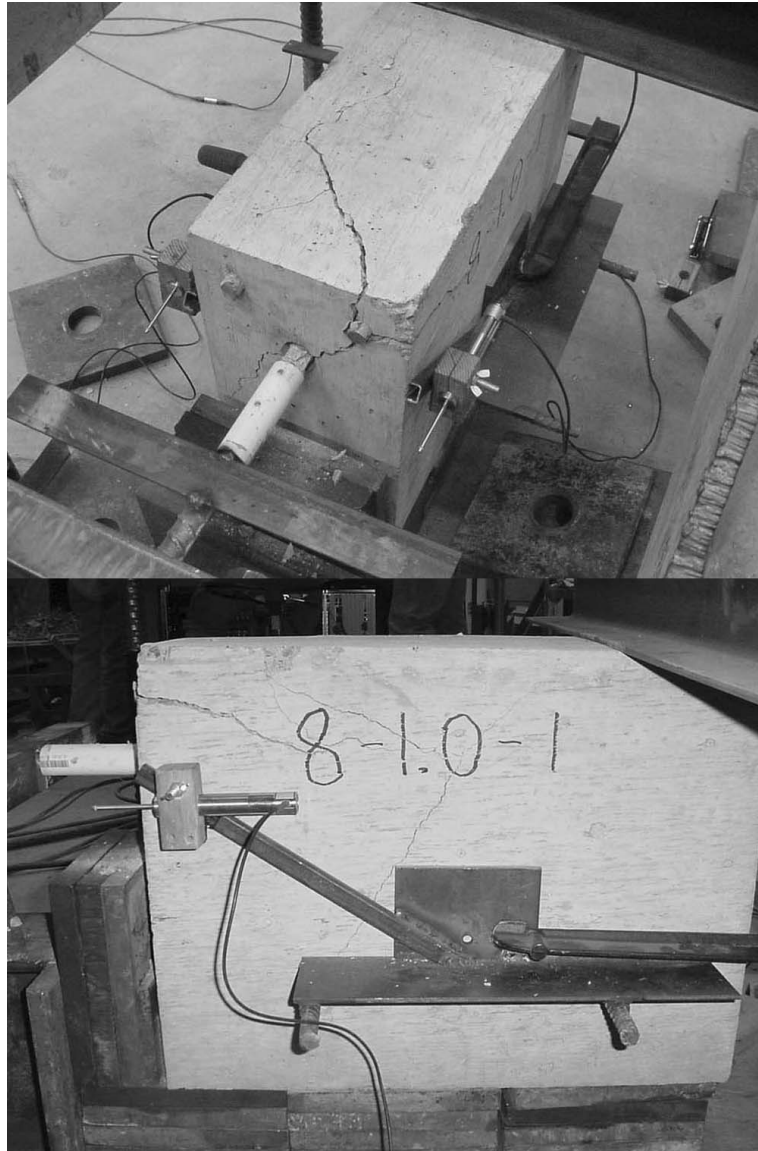


**Figure 3.16 Positioning of Loaded end LVDTs**

### **3.4.3 Specimen Modification**

In addition to the 72 specimens, two extra specimens were constructed for practice in using the testing apparatus. The extra specimens were constructed with #5 rebar as the test rebar. When the first of these two extra specimens was tested, the reinforcement fractured at the loaded end before bond failure occurred. After further evaluation the consensus was that the 8.5-in. bond length was sufficient to develop the fracture stress of the #5 rebar size. The bond length needed to be shortened in order for the specimen to experience bond failure. The solution was to drill cores in each of the #5 rebar-size specimens. Drilling core is shown in Figure 3.17. The diameters of the

cores were just large enough to envelop the reinforcement and surrounding PVC bond breaker. The cores were cut down the length of the reinforcement, effectively releasing a portion of the bond region. The new bond length for each of the #5 rebar-size specimens became 3.0 in. The second extra specimen was then tested and failure was due to bond as desired.

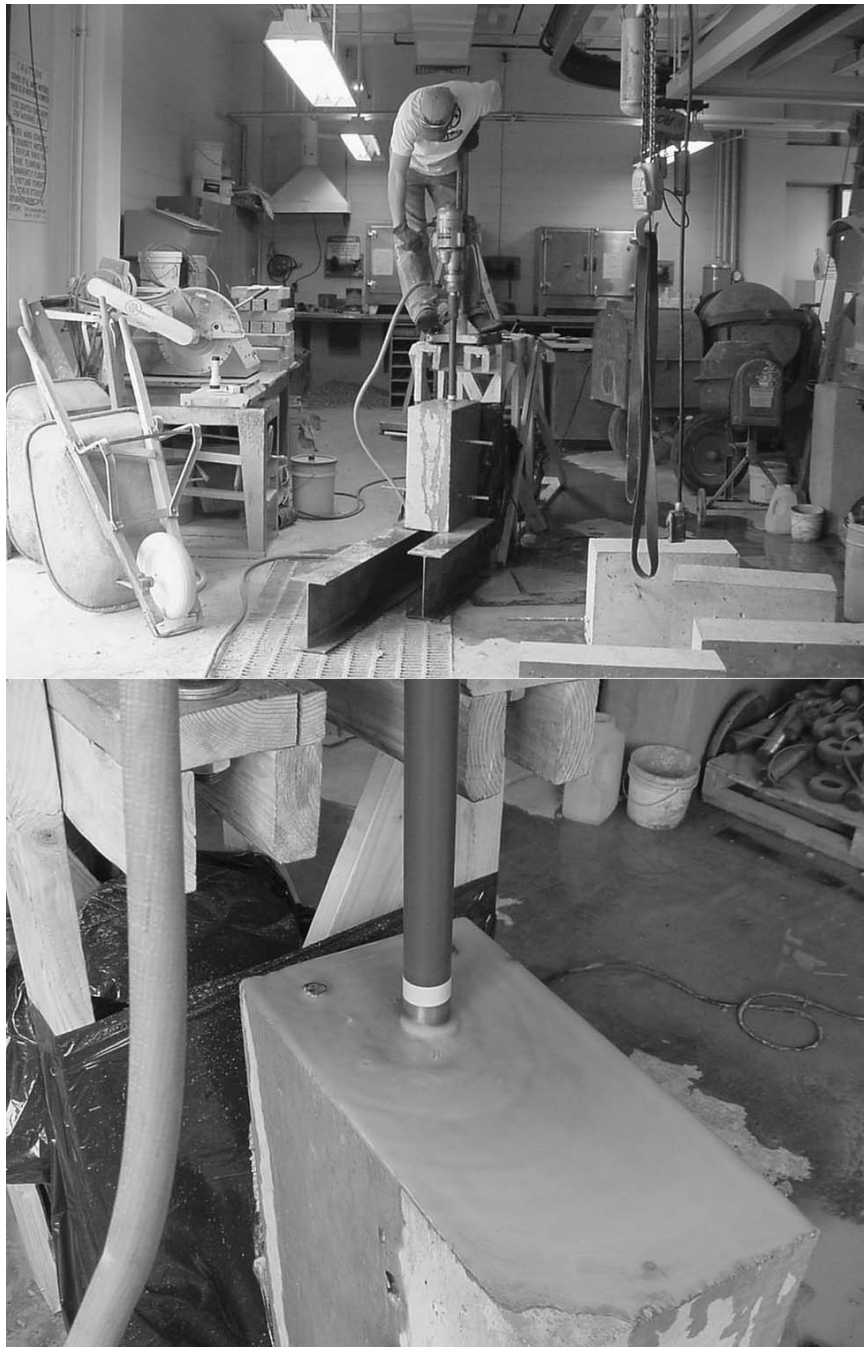


**Figure 3.17 Bond Length Adjustment of #5 Rebar Specimens**

## 4. Discussion of Results

### 4.1 Statistical Considerations

#### 4.1.1 Statistical Analysis Background

Data were analyzed using analysis of variance (ANOVA), Tukey's mean separation procedure, and bivariate linear regression. A brief explanation of these methods, as well as applicable terminology, is provided in this section.

#### ***Analysis of Variance (ANOVA)***

ANOVA is used to compare the means of three or more populations by considering a sample from each population of interest. ANOVA uses means and variances to determine if there is sufficient evidence to suggest that at least one of the means is different. Use of ANOVA requires two assumptions about the populations: populations are normally or nearly normally distributed and all populations have approximately equal variances, in other words, the squares of their standard deviations are approximately equal. ANOVA also requires two hypotheses: the null hypothesis or  $H_0$ , which indicates that the means of all considered populations are equal, and the alternative hypothesis or  $H_A$ , which indicates that the mean of at least one population is different from the means of the remaining populations (Hawley 1996, Moore 1995).

Within the ANOVA, the *F-statistic* ratio defined as the variation between samples divided by variation within samples is calculated. F-statistic ratios of or near one support the claim of the null hypothesis because ratios equal to one indicate that variation between samples is the same as that within samples. In contrast F-statistic ratios much greater than one support the claim of the alternative hypothesis (Hawley 1996).

ANOVA results are in terms of a p-value defined as the probability (assuming  $H_0$  is true for a population) that the test statistic would take a value as extreme or more extreme than the one actually observed. In the ANOVA the F-statistic is the test statistic. Generally, some value, e.g.,  $\alpha$ , is selected for comparison against the p-value in determining whether the test statistic is statistically significant or too extreme to be plausibly attributed to chance. The  $\alpha$  value essentially indicates a level of significance. For example, a  $\alpha$  value of 0.05 indicates a 0.05 level of significance or a result that occurs by chance only once in 20 experiments. Thus, for a  $\alpha$  value of 0.05, a p-value

less than 0.05 indicates that the probability of obtaining the test statistic value is less than 5% when the null hypothesis is true. The null hypothesis is therefore rejected because such results is said to be too extreme to be attributed to chance. If, however, the p-value is greater than 0.05 there is insufficient evidence to reject the null hypothesis (Moore 1995).

### ***Tukey's Mean Separation Procedure***

The Tukey test identifies which pairs of population means are significantly different in contrast to the ANOVA which is indicative of the difference of at least one population mean from the others but does not reveal which means are different. Based on a specified level of significance,  $\alpha$ , the Tukey test is used to calculate the limits for the differences of individual means when compared pair-wise. If the calculated limits for a particular pair span zero, i.e., the limits have opposite signs, then there is a possibility that there is zero difference between the pair. Therefore, there is not sufficient evidence to conclude that the pair is significantly different at the given level of significance. If the calculated limits, however, for a particular pair do not span zero, i.e., the limits have the same sign, then there is sufficient evidence to conclude that the pair is significantly different (Rowe 2003).

### ***Bivariate Linear Regression***

The bivariate linear regression method indicates how some response variable,  $y$ , is related to some predictor, or control variable,  $x$ , i.e., how  $y$  is affected by changes in  $x$ . The method uses the line, given in Eq. 4.1, which best fits all the collected data points in an experiment as the indicator of how  $y$  is affected by changes in  $x$ .

$$y = mx + b \dots\dots\dots(\text{Eq. 4.1})$$

Where:

$y$ : Response variable

$x$ : Predictor variable

$m$ : Slope

$b$ : The  $y$  intercept, or the value of  $y$  when  $x$  is zero.

Values for  $m$  and  $b$  are calculated using the least-squares regression method, which involves minimizing the sum of the squared error terms for a candidate line. An

*error term* is the distance, in the  $y$  direction, between a data point and the prospective line (Moore 1995).

The bivariate linear regression yields a value called *the coefficient of determination*, or  $R^2$ , which is the proportion of the variance of  $y$  that is explained by the variance of  $x$ .  $R^2$  is a value always between zero and one. A high  $R^2$  value indicates that the predictor variable explains a high percentage of the response variable variation, and vice versa (Hamilton 1992).

A *p-value* is also calculated to determine if the observed relationship between predictor and response variables is statistically significant. As mentioned previously a  $p$ -value less than a chosen  $\alpha$  indicates sufficient evidence to reject the null hypothesis. For the bivariate linear regression method the null hypothesis states that the slope,  $m$ , is zero for the linear regression under consideration. A zero slope indicates there is no correlation between the predictor and response variables

#### **4.1.2 Experimental Design Mitigation**

A lack of randomization in the assignment of treatments to experimental units in the experimental design was observed. As described earlier, bar size and corrosion treatments were assigned such that half the possible corrosion level treatments and a single bar size treatment were cast at the same time. The lack of randomization made concrete strength a potential covariate in the experiment. A covariate is a source of variance that is thought to influence the response variable, but has not been controlled by the experimental procedure (Rutherford 2001). A covariate is said to be confounded with the predictor variable. In other words, the effect the predictor variable has on the response variable cannot be distinguished from the effect the covariate has on the response variable (Moore 1995). The covariate, concrete strength, was confounded with two predictor variables, corrosion level and bar size.

Two approaches were used to mitigate the experimental design error. The first approach was to divide the experiment into three separate studies, differentiated by bar size. Such an approach served to nullify the effects of differences of concrete strength between bar sizes. The approach also made sense due to the fact that the bond length of the #5 rebar specimens had been reduced to only 3 in., while the bond lengths of the #8 and #11 rebar specimens remained at 8.5 in.

The second approach involved comparing the concrete strength of the two casts within a bar group. Concrete cores for use in determining concrete strength were

therefore drilled from test specimens from all six cast groups following the pull-out testing. The cores were chosen over the previously cast cylinders because the cores were thought to give a more accurate representation of concrete compressive strength of individual specimens. Furthermore, the cast cylinders underwent slightly different curing conditions than the actual test specimens. Accordingly, the cores were cut and capped according to the cylinder specifications of ASTM C31. Cores were tested in compression on a Baldwin hydraulic machine at a constant strain rate of 0.01 in./min. ANOVA was used to analyze the data and p-values for the #5, #8, and #11 rebars were 0.514, 0.806, and 0.277, respectively. Since p-values were greater than the selected value of 0.05 for  $\alpha$ , there was insufficient evidence to reject the null hypotheses that the concrete strengths of specimens within a bar size were equal; concrete strengths therefore were considered to be equal for a rebar size. Thus concrete strength was no longer a covariate in the experiment.

Data analyses presented in this report are therefore based on the premise that concrete strength did not vary significantly between specimens of a particular rebar size.

## 4.2 Maximum Load

### 4.2.1 Results

Figure 4.1 shows a typical load-versus-slip diagram.

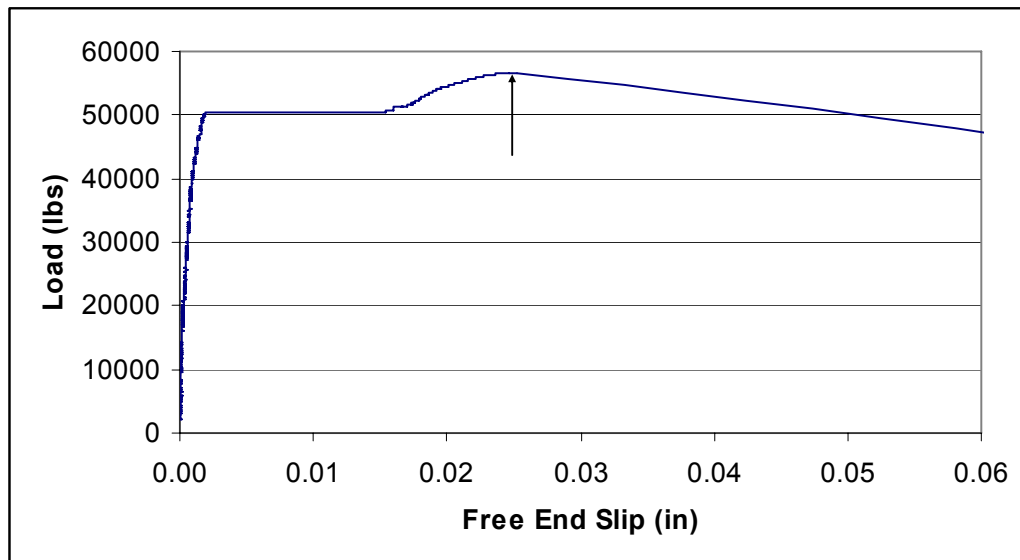


Figure 4.1 Load vs. Slip Diagram - Specimen 8-0.25-3

Load-versus-slip diagrams were plotted and maximum load reached was determined for every test specimen. Maximum load is presented in Table 4.1. In the specimen name designation the first number designates the bar size, the second number designates the target percent corrosion, and the third designates the replicate number.

**Table 4.1 Maximum Load (lbs.)**

Specimen Name	Maximum Load	Specimen Name	Maximum Load	Specimen Name	Maximum Load
5-0.00-1	22206	8-0.00-1	57622	11-0.00-1	55218
5-0.00-2	23752	8-0.00-2	59665	11-0.00-2	54013
5-0.00-3	23467	8-0.00-3	59102	11-0.00-3	53768
5-0.25-1	24263	8-0.25-1	53209	11-0.25-1	64177
5-0.25-2	24655	8-0.25-2	63083	11-0.25-2	54639
5-0.25-3	21367	8-0.25-3	56603	11-0.25-3	58348
5-0.50-1	23577	8-0.50-1	68522	11-0.50-1	54431
5-0.50-2	19807	8-0.50-2	57734	11-0.50-2	61109
5-0.50-3	23301	8-0.50-3	54113	11-0.50-3	59056
5-1.00-1	20439	8-1.00-1	68763	11-1.00-1	56172
5-1.00-2	16570	8-1.00-2	58569	11-1.00-2	54621
5-1.00-3	20867	8-1.00-3	53195	11-1.00-3	55593
5-2.00-1	24610	8-2.00-1	64249	11-2.00-1	52569
5-2.00-2	26370	8-2.00-2	57710	11-2.00-2	52291
5-2.00-3	23922	8-2.00-3	62314	11-2.00-3	54321
5-5.00-1	23443	8-5.00-1	52870	11-5.00-1	55287
5-5.00-2	20948	8-5.00-2	60300	11-5.00-2	61809
5-5.00-3	25076	8-5.00-3	64709	11-5.00-3	54166
5-7.50-1	26527	8-7.50-1	49501	11-7.50-1	56807
5-7.50-2	23578	8-7.50-2	55568	11-7.50-2	52407
5-7.50-3	21678	8-7.50-3	66081	11-7.50-3	57766
5-10.00-1	22013	8-10.00-1	55506	11-10.00-1	55141
5-10.00-2	21387	8-10.00-2	59909	11-10.00-2	51048
5-10.00-3	21293	8-10.00-3	61755	11-10.00-3	58315

Results from analyses are summarized in Table 4.2. The level of significance  $\alpha$  for all analyses was 0.05.

An ANOVA was performed on the maximum load data. The analysis compared the maximum loads of all sets of corrosion levels for a given rebar size and determined if the maximum load achieved for at least one set was significantly different from the rest. The analysis indicates that the #5 rebar specimens had at least one set significantly different from the rest while the #8 and #11 rebar specimens did not.

A Tukey test was then performed on the #5 rebar data to determine which corrosion levels yielded significant differences. The Tukey test pairs, presented on Table 4.2, indicate a significant difference between the 1.0% and 2.0% corrosion levels.

Finally, a bivariate linear regression was performed. Plots of maximum load versus percent bar corrosion for the #5, #8, and #11 rebar specimens are shown in Figures 4.2 to 4.4, respectively. The calculated linear regression lines are plotted amongst the data points. Linear regression  $R^2$  values, p-values, and line equations are tabulated in Table 4.2 and are also included on Figures 4.2 to 4.4.

Close inspection of Figures 4.2 to 4.4 reveal that data points are not aligned exactly at the specified target corrosion levels. The reason for the discrepancy is that all linear regression plots used actual rather than specified percent corrosion levels.

**Table 4.2 Statistical Analysis Results for Maximum Load**

Rebar Size		#5	#8	#11
ANOVA	P-Value	0.045	0.987	0.315
Tukey Test	Pairs	1.0-2.0	n/a	n/a
Linear Regression	P-Value	0.926	0.703	0.505
	$R^2$	0.0004	0.0067	0.0205
	Slope	11.863	-110.28	-121.62
	Y-Intercept	22665	59628	56416

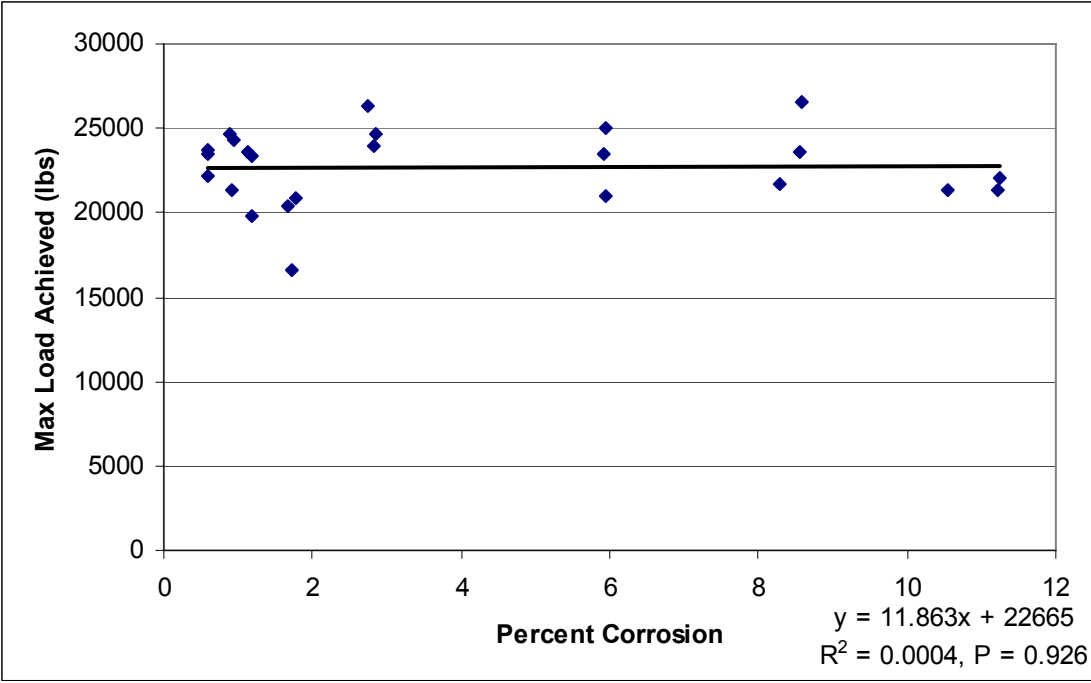


Figure 4.2 Maximum Load vs. Percent Corrosion for #5 Rebar Specimens

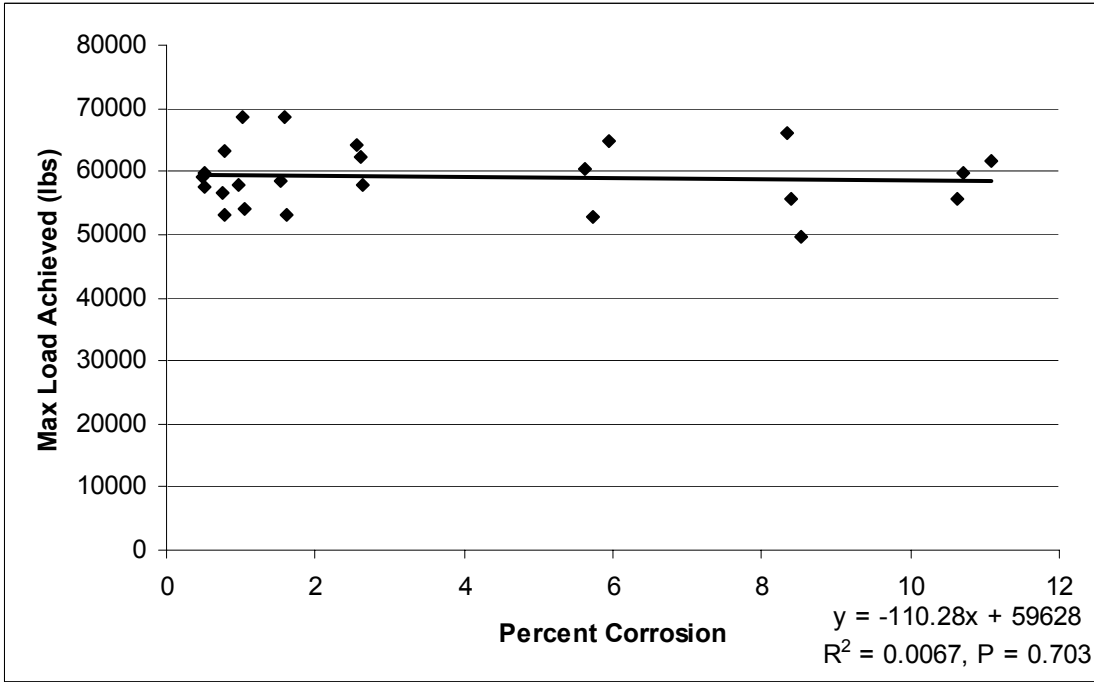
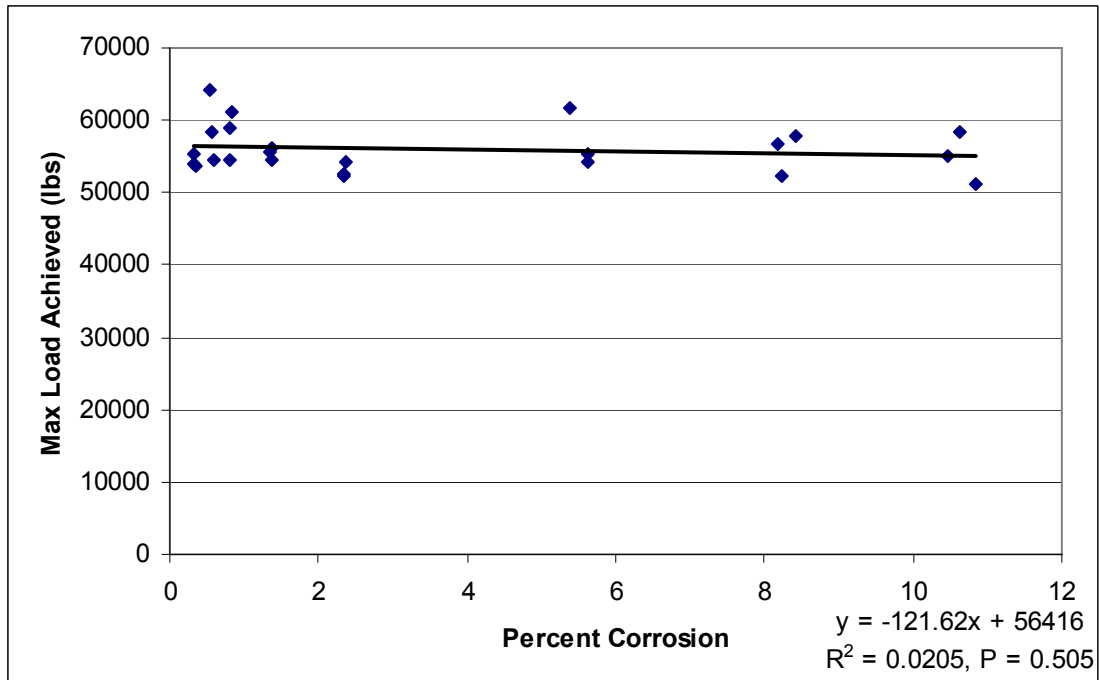


Figure 4.3 Maximum Load vs. Percent Corrosion for #8 Rebar Specimens



**Figure 4.4 Maximum Load vs. Percent Corrosion for #11 Rebar Specimens**

The linear regression p-values of all three rebar sizes far exceed the selected 0.05 level of significance. Therefore, there is insufficient evidence to reject the null hypothesis that the slope of the regression lines for the respective populations of specimens is zero. Regression lines shown in Figures 4.2 to 4.4 were calculated from samples obtained from a #5 rebar specimen population, a #8 rebar specimen population, and a #11 rebar specimen population, respectively. Thus, the notion of “population” as presented here is a theoretical one and refers to an infinite number of potentially existing specimens at a given bar size. Thus, while the slopes of the regression lines for the samples may be non-zero, there is insufficient evidence to show the slopes of the regression lines for the populations are non-zero. Lower p-values and therefore greater statistical evidence would be obtained if there were less spread of maximum load values at a given corrosion level and if the magnitude of the regression line slope was greater.

#### **4.2.2 Discussion**

The initial hypothesis of this study was that increased corrosion decreases maximum load. Results of the statistical analysis are insufficient to support this hypothesis. Darwin and Graham (1993) determined that maximum load decreased with a decrease in the relative rib area. The initial hypothesis of this study was based on the

assumption that corrosion essentially reduces the relative rib area, therefore reducing the maximum load.

One possible explanation for the findings of this study is that corrosion does not significantly alter the relative rib area. Two factors decrease the relative rib area for a given bar size: (1) a decrease in the projected rib area normal to the bar and (2) an increase in the center-to-center rib spacing. Corrosion decreases the projected rib area but further consideration must be given to the effect on center-to-center rib spacing. Figure 4.5 shows the eight levels of corrosion considered in this study for #8 rebar specimens. Additional pitting forms between ribs as corrosion progresses. The peaks and valleys of the additional pitting could, themselves, serve the same purpose as the original ribs, providing interlock between the concrete and steel. The additional “pit-ribbing” could effectively reduce the center-to-center spacing of the ribs and offset reductions in projected rib area, thereby maintaining the same relative rib area even as corrosion progresses. Therefore because of offsetting effects non-corroded and corroded rebars may have similar maximum pull-out loads. Thus, the hypothesis that increased corrosion decreases maximum load may not be reasonable because of corrosions’ offsetting effects.

The failure mode of the specimens provides additional evidence of continued rib-concrete interaction for corroded bar. Figure 4.6 shows two #8 rebar specimens after testing. Specimen 8-0.00-2, top specimen, is a 0.0% target corrosion level, while the specimen 8-10.0-3, bottom specimens, is a 10.0% target corrosion level. Typical failure modes were splitting failures. Essentially the tensile capacity of the concrete was exceeded due to tensile stresses generated by the force which the rebar ribs (or additional “pit-ribbing” caused by the corrosion) exerted on the concrete. Darwin and Graham (1993) observed similar failure of specimens cast without transverse shear reinforcement. The observed failure mode in the highly corroded bars suggests that original rib- or corrosion originated rib-concrete interaction is, indeed, occurring. Figure 4.7 shows similar failure modes for #11 rebar specimens.

The brittle splitting failure of the specimens may explain the unchanging maximum load response and, therefore, may be another covariate masking the effects of the corrosion. Although the brittle splitting failure may, indeed, have some effect, none of the #5 rebar specimens experienced such cracking. Failure of #5 rebar specimens was completely localized to the interface between concrete and reinforcement. Figure 4.8 shows the localized failure typical of all #5 bar specimens. Even though typical

failure mode for #5 rebar specimens were different than that of #8 and #11 rebar specimens, they still experienced unchanging maximum load response with increased corrosion. Brittle splitting cracking is not the sole contributor, and due to the observation just described may not be a contributor at all to the unchanging maximum load response behavior.

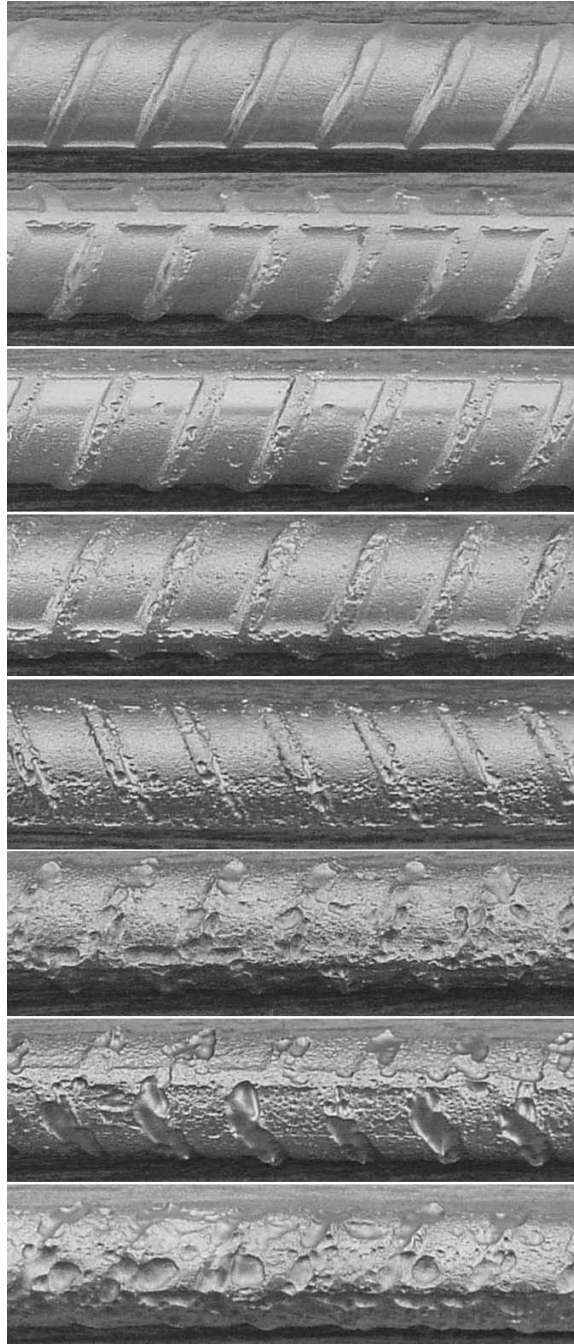


**Figure 4.5 Levels of Corrosion Considered in this Study (#8 Rebars Shown)**

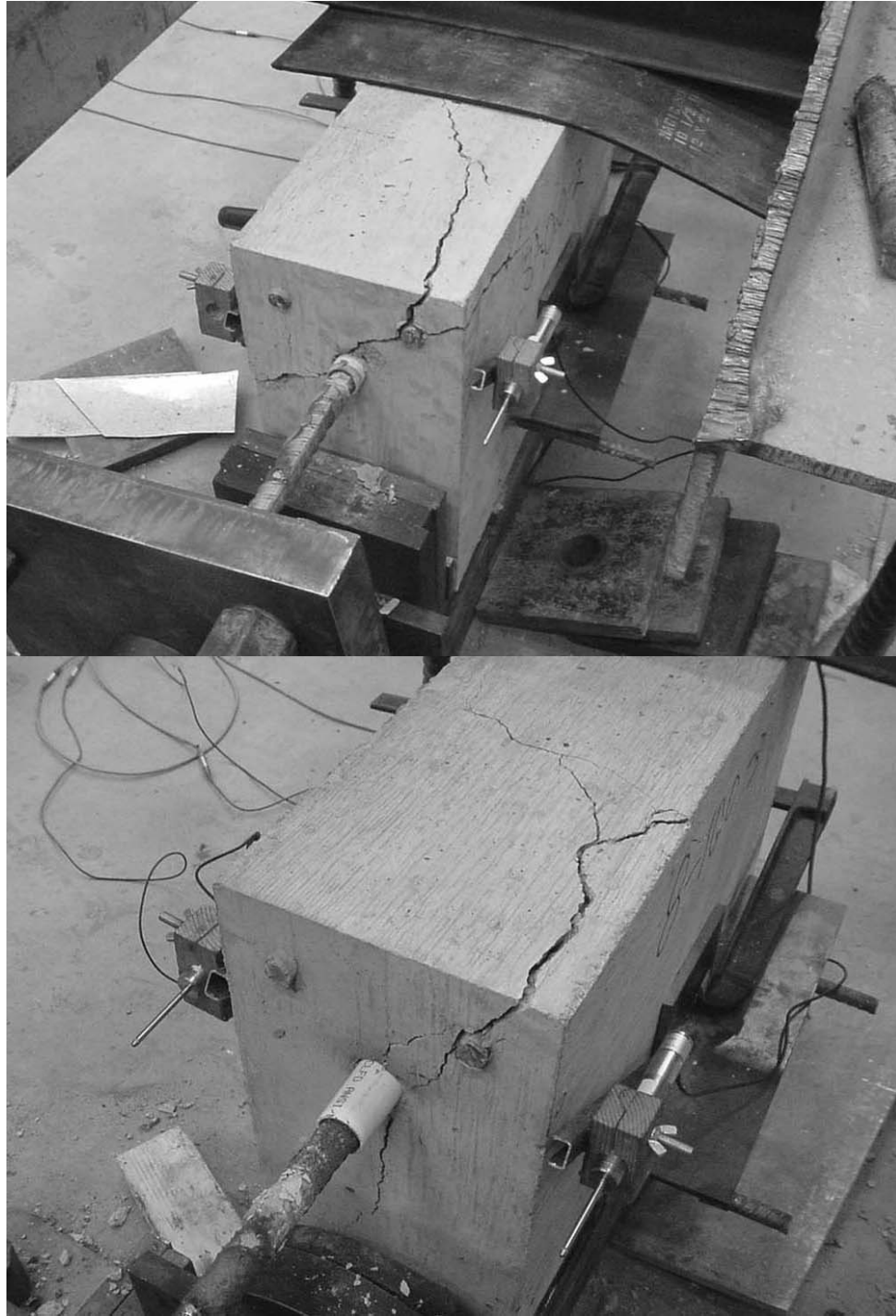


**Figure 4.6 Typical Failure Mode of #8 Rebar Specimens  
(Specimens 8-00-2 and 8-10.0-3, Top and Bottom, Respectively)**

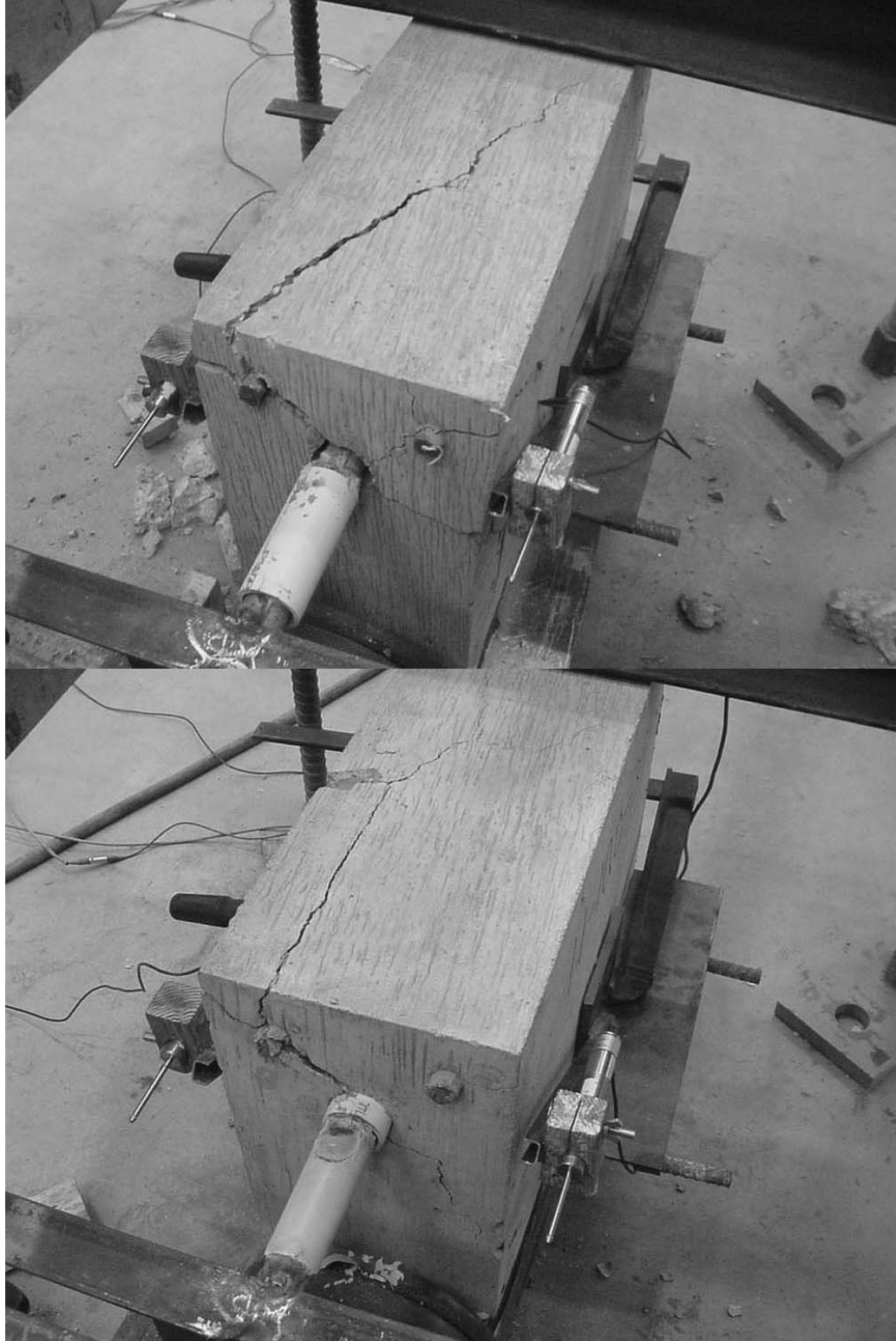


**Figure 4.7 Typical Failure Mode of #11 Rebar Specimens  
(Specimens 11-0.00-3 and 11-10.0-3, Top and Bottom, Respectively)**

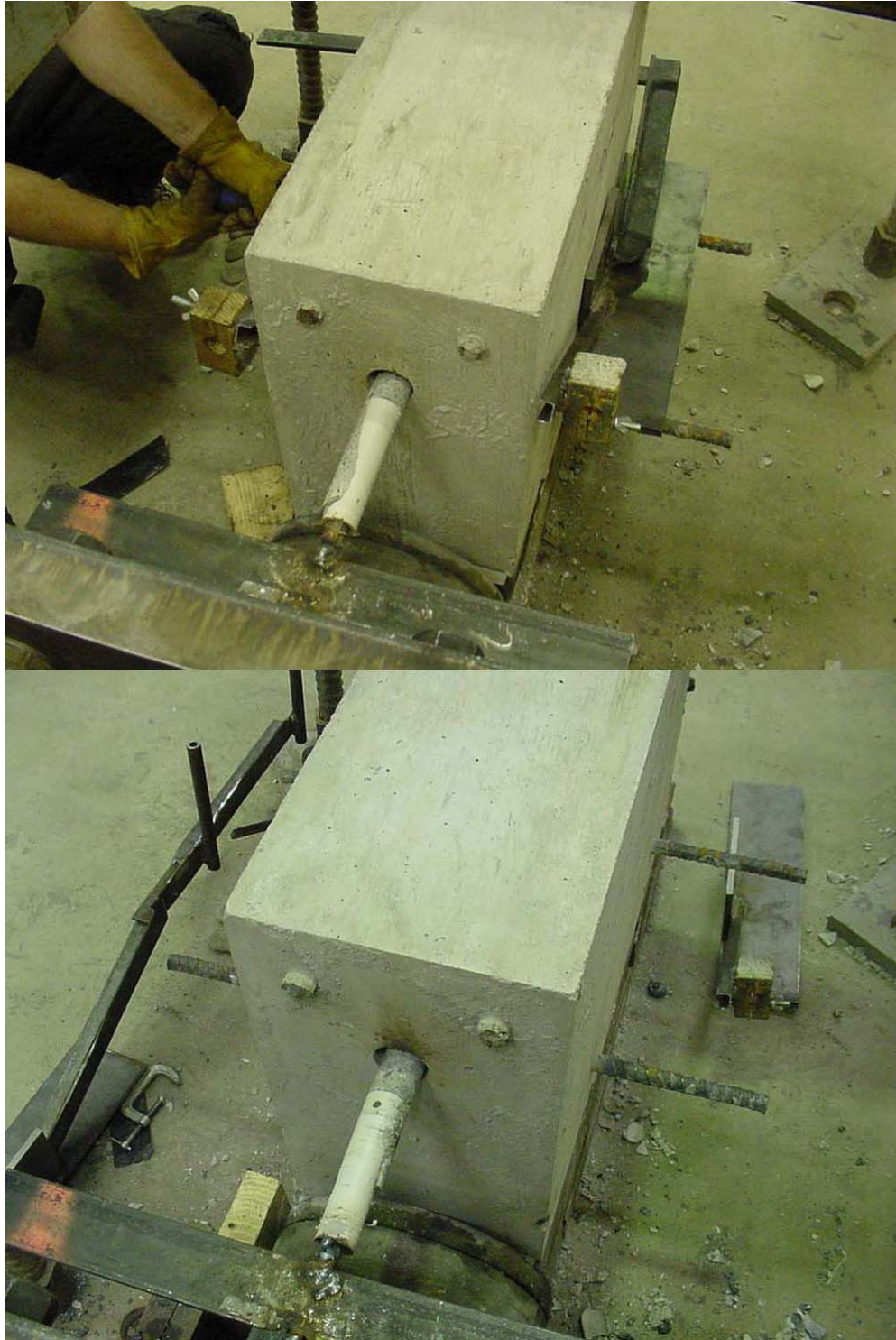


**Figure 4.8 Typical Failure Mode of #5 Rebar Specimens  
(Specimens 5-0.00-1 and 5-10.0-3, Top and Bottom, Respectively)**

### 4.3 Initial Slip Load

#### 4.3.1 Results

Figure 4.9 shows a graphical representation of the initial slip load, which is being defined as the load at which noticeable slip occurred followed by continued load increase. Initial slip load is not applicable to the #5 rebar specimens because all #5 rebar specimens exhibited no distinguishable point of initial slip, but exhibited a more gradual slip. Figure 4.10 shows a typical load-versus-slip diagram for a #5 rebar specimen. The initial slip load was determined from numerical data and is summarized in Table 4.3.

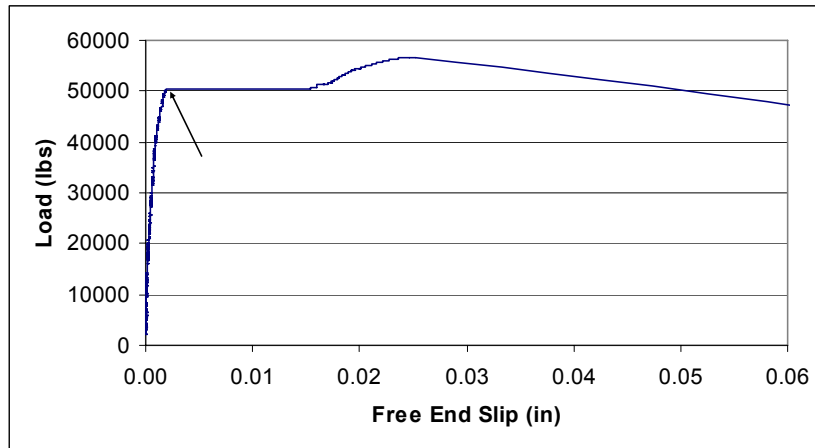


Figure 4.9 Initial Slip Load from Load vs. Slip Diagram - Specimen 8-0.25-3

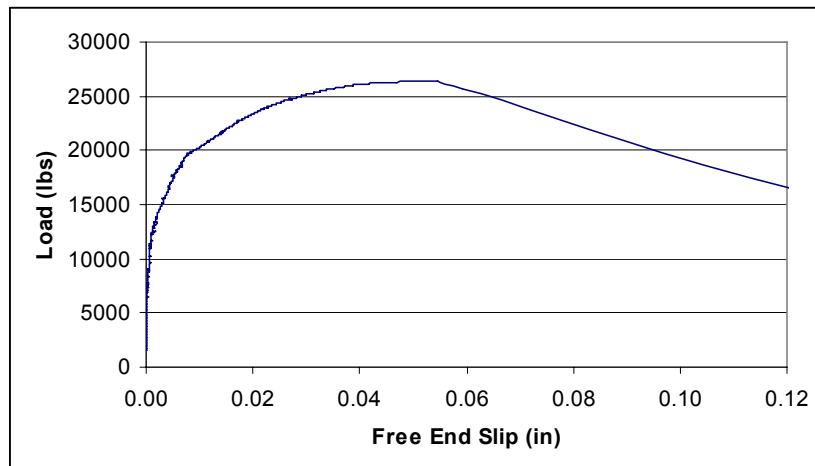


Figure 4.10 Typical #5 Rebar Specimen Load vs. Slip Diagram

**Table 4.3 Initial Slip Load (lbs.)**

Specimen Name	Initial Slip Load	Specimen Name	Initial Slip Load	Specimen Name	Initial Slip Load
5-0.00-1	n/a	8-0.00-1	52830	11-0.00-1	55157
5-0.00-2	n/a	8-0.00-2	57673	11-0.00-2	49783
5-0.00-3	n/a	8-0.00-3	53606	11-0.00-3	52201
5-0.25-1	n/a	8-0.25-1	46506	11-0.25-1	48526
5-0.25-2	n/a	8-0.25-2	60152	11-0.25-2	53661
5-0.25-3	n/a	8-0.25-3	50297	11-0.25-3	54082
5-0.50-1	n/a	8-0.50-1	54970	11-0.50-1	48207
5-0.50-2	n/a	8-0.50-2	48328	11-0.50-2	53463
5-0.50-3	n/a	8-0.50-3	51800	11-0.50-3	50396
5-1.00-1	n/a	8-1.00-1	53868	11-1.00-1	48168
5-1.00-2	n/a	8-1.00-2	52729	11-1.00-2	47738
5-1.00-3	n/a	8-1.00-3	52624	11-1.00-3	55425
5-2.00-1	n/a	8-2.00-1	53107	11-2.00-1	44876
5-2.00-2	n/a	8-2.00-2	53472	11-2.00-2	47123
5-2.00-3	n/a	8-2.00-3	52372	11-2.00-3	46977
5-5.00-1	n/a	8-5.00-1	41310	11-5.00-1	42825
5-5.00-2	n/a	8-5.00-2	53275	11-5.00-2	49766
5-5.00-3	n/a	8-5.00-3	54186	11-5.00-3	46419
5-7.50-1	n/a	8-7.50-1	48472	11-7.50-1	41309
5-7.50-2	n/a	8-7.50-2	51754	11-7.50-2	44572
5-7.50-3	n/a	8-7.50-3	52794	11-7.50-3	41376
5-10.00-1	n/a	8-10.00-1	48232	11-10.00-1	49407
5-10.00-2	n/a	8-10.00-2	47420	11-10.00-2	46215
5-10.00-3	n/a	8-10.00-3	54223	11-10.00-3	52770

An ANOVA was first performed on the initial slip load data and p-values are listed in Table 4.4. The analysis results indicates that #11 rebar specimens had at least one set significantly different from the rest; #8 rebar specimens did not.

**Table 4.4 Statistical Analysis Results for Initial Slip Load**

Bar Size		#5	#8	#11
ANOVA	P-Value	n/a	0.816	0.01
Tukey Test	Pairs	n/a	n/a	0.0-7.5, 0.25-7.5
Linear Regression	P-Value	n/a	0.127	0.016
	R <sup>2</sup>	n/a	0.1026	0.2359
	Slope	n/a	-327.25	-529.88
	Y-Intercept	n/a	53203	50749

The Tukey test results indicate a significant difference in the initial slip load response between 0.0% and 7.5% corrosion levels for #5 rebar specimens and between 0.25% and 7.5% corrosion levels for #11 rebar specimens.

Plots of the bivariate linear regression for initial slip load versus percent bar corrosion for the #8 and #11 rebar specimens are shown in Figures 4.11 and 4.12, respectively. The calculated linear regression lines are plotted amongst the data points. Linear regression R<sup>2</sup> values, p-values, and line equations are included on the figures and summarized in Table 4.4.

The linear regression p-value for the #8 rebar specimens exceeds the 0.05 level of significance, indicating insufficient evidence to reject the null hypothesis. The linear regression p-value for the #11 rebar specimens, however, is less than the 0.05 level of significance, indicating sufficient evidence to reject H<sub>0</sub>. In other words, there is a relationship between corrosion level and initial slip load for the #11 rebar specimens. Increases in corrosion result in a decrease in initial slip load for #11 rebar specimens. The R<sup>2</sup> value indicates that variation in corrosion accounts for 23.6% of variation in initial slip load. Accordingly every one percent increase in corrosion results in a decrease in initial slip load of approximately 530 pounds.

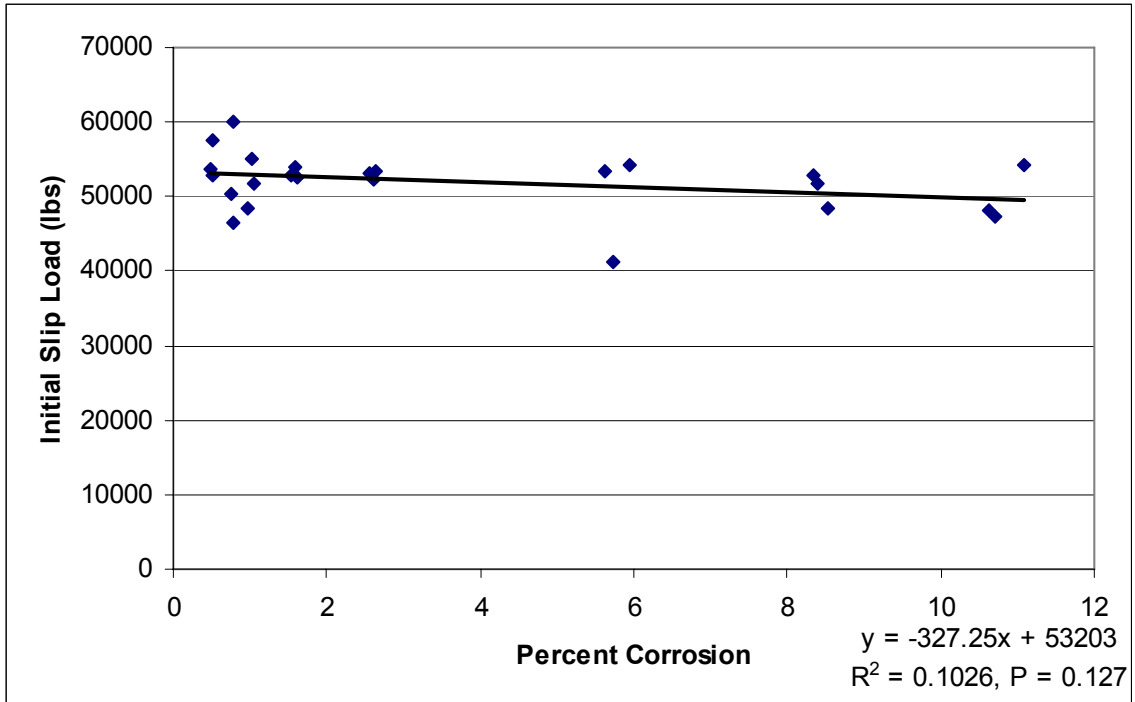


Figure 4.11 Initial Slip Load vs. Percent Corrosion for #8 Bar Specimens

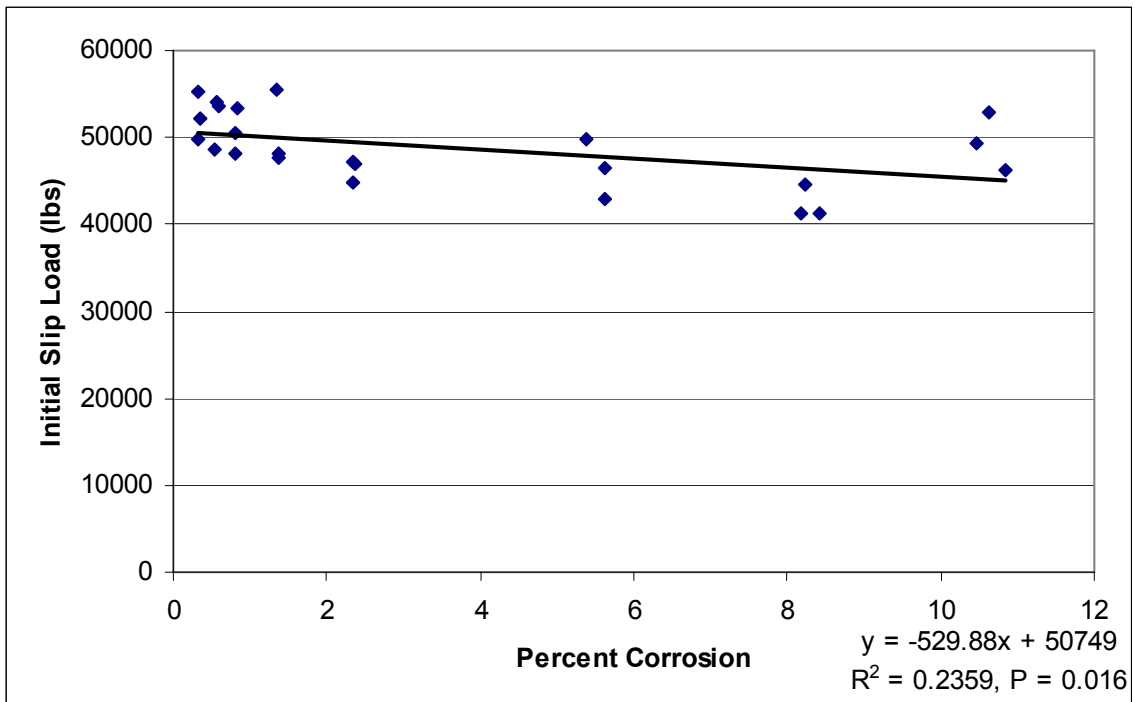


Figure 4.12 Initial Slip Load vs. Percent Corrosion for #11 Bar Specimens

### 4.3.2 Discussion

A different pull-out behavior between rebar sizes was observed. The #5 rebar specimens exhibited a gradual increase in pullout while both the #8 and #11 rebar specimens experienced an initial slip followed by continued load-carrying capacity. Two factors may have contributed to such a behavior: bond lengths and failure modes

Bond lengths of #5 rebar specimens were shorter than those of #8 and #11 rebar specimens and perhaps the bond interaction for shorter bond lengths lends itself more to gradual slippage. Additional testing of #8 and #11 rebar specimens with shorter bond lengths would be required to verify hypothesis.

The failure mode of #5 rebar specimens differed from that of larger rebar specimens. The #5 rebar specimens exhibited localized crushing at the bond interface while the larger rebar specimens exhibited brittle cracking which may be attributed to the relative size of the rebars compared to the size of the concrete block in which they were embedded. Thus, for a given load, it is plausible that a larger rebar would generate greater splitting stress than a smaller rebar. Perhaps the initial slip of larger rebars occurred when splitting stresses immediately around the rebar exceeded the tensile capacity of concrete; thus reducing the confining pressure and allowing the rebar to slip.

The increase in rebar corrosion may have had an effect on the initial slip load, such as facilitating local crushing of the concrete, due to reduced rebar rib height. The bearing pressure on the concrete that engages the ribs is most likely increased due to a reduction in the rib area normal to the bar axis. As corrosion increases, rib height decreases, rib area decreases, and the bearing pressure on the concrete increases. Eventually the localized bearing point crushes and slippage occurs. The ability to still support further load after initial slip comes as the crushed concrete in front of the ribs is compressed against intact material along the slip path.

The linear regression p-value for the #8 rebar specimens slightly exceeds the 0.05 level of significance. Increased sampling may have resulted in a statistically significant regression line. Another way to obtain statistically significant regression lines for both #8 and #11 rebar sizes would be to compute higher order regression lines. Both sets of data lend themselves to quadratic functions. However, beyond improving the quality of the curve-fitting there is no theoretical reason to believe that initial slip load would have a quadratic relationship with corrosion. For this reason, quadratic plots have not been generated in this study.

## 4.4 Slip Prior to Failure

### 4.4.1 Results

Figure 4.13 shows a graphical representation of the slip prior to failure. Slip prior to failure is defined as the amount of free end slip that occurs between initiation of loading and complete bond failure. Complete bond failure is the point at which the bar is released from the block. According to Figure 4.13, specimen 8-0.25-3 experienced nearly 0.025 inch of slip prior to bond failure. Slip was determined from numerical data and is listed in Table 4.5 for every specimen.

An ANOVA was first performed on the data. The ANOVA p-values listed in Table 4.6 indicate the #5 rebar specimens had at least one set significantly different from the rest, while neither the #8 rebar specimens nor the #11 rebar specimens had significant differences in slip due to the corrosion treatments.

The Tukey test pairs indicate a significant difference in the slip prior to failure response between 0.0% and 10.0% corrosion and 0.25% and 10.0% corrosion for the #5 rebar specimens. These results indicate that differences exist between extreme ends of corrosion level

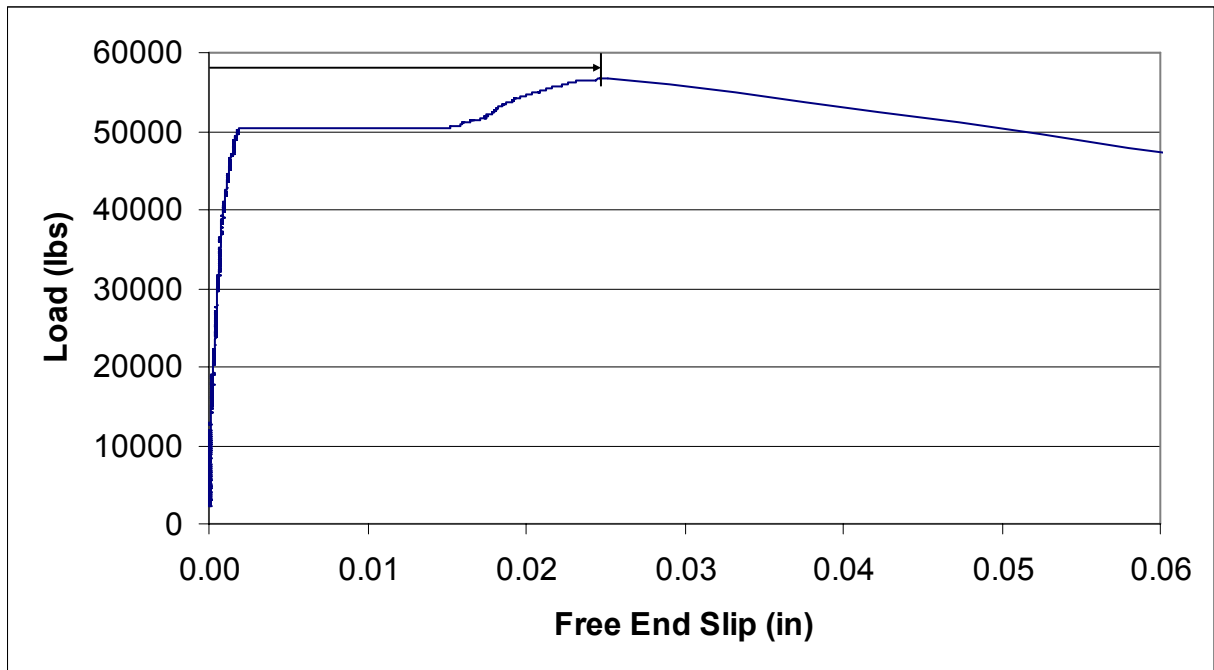


**Figure 4.13 Determination of Slip Prior to Failure from Load vs. Slip Diagram (Specimen 8-0.25-3 Shown)**

**Table 4.5 Slip Prior to Failure (in.)**

Specimen Name	Slip Prior to Failure	Specimen Name	Slip Prior to Failure	Specimen Name	Slip Prior to Failure
5-0.00-1	0.0416	8-0.00-1	0.0241	11-0.00-1	0.0235
5-0.00-2	0.0364	8-0.00-2	0.0299	11-0.00-2	0.0238
5-0.00-3	0.0579	8-0.00-3	0.0240	11-0.00-3	0.0273
5-0.25-1	0.0441	8-0.25-1	0.0141	11-0.25-1	0.0280
5-0.25-2	0.0425	8-0.25-2	0.0426	11-0.25-2	0.0237
5-0.25-3	0.0485	8-0.25-3	0.0252	11-0.25-3	0.0281
5-0.50-1	0.0532	8-0.50-1	0.0296	11-0.50-1	0.0283
5-0.50-2	0.0415	8-0.50-2	0.0211	11-0.50-2	0.0231
5-0.50-3	0.0536	8-0.50-3	0.0277	11-0.50-3	0.0325
5-1.00-1	0.0609	8-1.00-1	0.0402	11-1.00-1	0.0305
5-1.00-2	0.0546	8-1.00-2	0.0332	11-1.00-2	0.0268
5-1.00-3	0.0529	8-1.00-3	0.0282	11-1.00-3	0.0294
5-2.00-1	0.0530	8-2.00-1	0.0354	11-2.00-1	0.0297
5-2.00-2	0.0545	8-2.00-2	0.0386	11-2.00-2	0.0271
5-2.00-3	0.0612	8-2.00-3	0.0324	11-2.00-3	0.0255
5-5.00-1	0.0648	8-5.00-1	0.0263	11-5.00-1	0.0354
5-5.00-2	0.0642	8-5.00-2	0.0345	11-5.00-2	0.0018
5-5.00-3	0.0708	8-5.00-3	0.0444	11-5.00-3	0.0254
5-7.50-1	0.0840	8-7.50-1	0.0367	11-7.50-1	0.0310
5-7.50-2	0.0816	8-7.50-2	0.0305	11-7.50-2	0.0332
5-7.50-3	0.0643	8-7.50-3	0.0386	11-7.50-3	0.0271
5-10.00-1	0.0549	8-10.00-1	0.0184	11-10.00-1	0.0314
5-10.00-2	0.0771	8-10.00-2	0.0324	11-10.00-2	0.0307
5-10.00-3	0.1152	8-10.00-3	0.0414	11-10.00-3	0.0249

**Table 4.6 Statistical Analysis Results for Slip Prior to Failure**

Bar Size		#5	#8	#11
ANOVA	P-Value	0.013	0.582	0.75
Tukey Test	Pairs	0.0-10.0, 0.25-10.0	n/a	n/a
Linear Regression	P-Value	0.000	0.230	0.605
	R <sup>2</sup>	0.5814	0.0649	0.0123
	Slope	0.0035	0.0005	0.0002
	Y-Intercept	0.0455	0.0291	0.0263

Plots of the bivariate linear regression for slip prior to failure versus percent bar corrosion were generated and are shown in Figures 4.14 to 4.16 for #5, #8, and #11 rebar specimens, respectively. The calculated linear regression lines are plotted amongst the data points. Linear regression  $R^2$  values, p-values, and line equations are included on the figures and tabulated in Table 4.6.

The linear regression p-value for the #8 and #11 rebar specimens exceeds the 0.05 level of significance, indicating insufficient evidence to reject the null hypothesis. In other words, there is insufficient evidence to disprove that the slope of the regression is zero and the resultant notion that there is no relationship between corrosion level and slip prior to failure. The linear regression p-value for the #5 rebar specimens, however, is less than the 0.05 level of significance, indicating sufficient evidence to reject the null hypothesis. Increases in corrosion are shown to increase the amount of slip prior to failure. The  $R^2$  value indicates that variation in corrosion accounts for 58.1% of variation in slip prior to failure. Accordingly, every one percent increase in corrosion increases slip prior to failure by 0.0035 in.

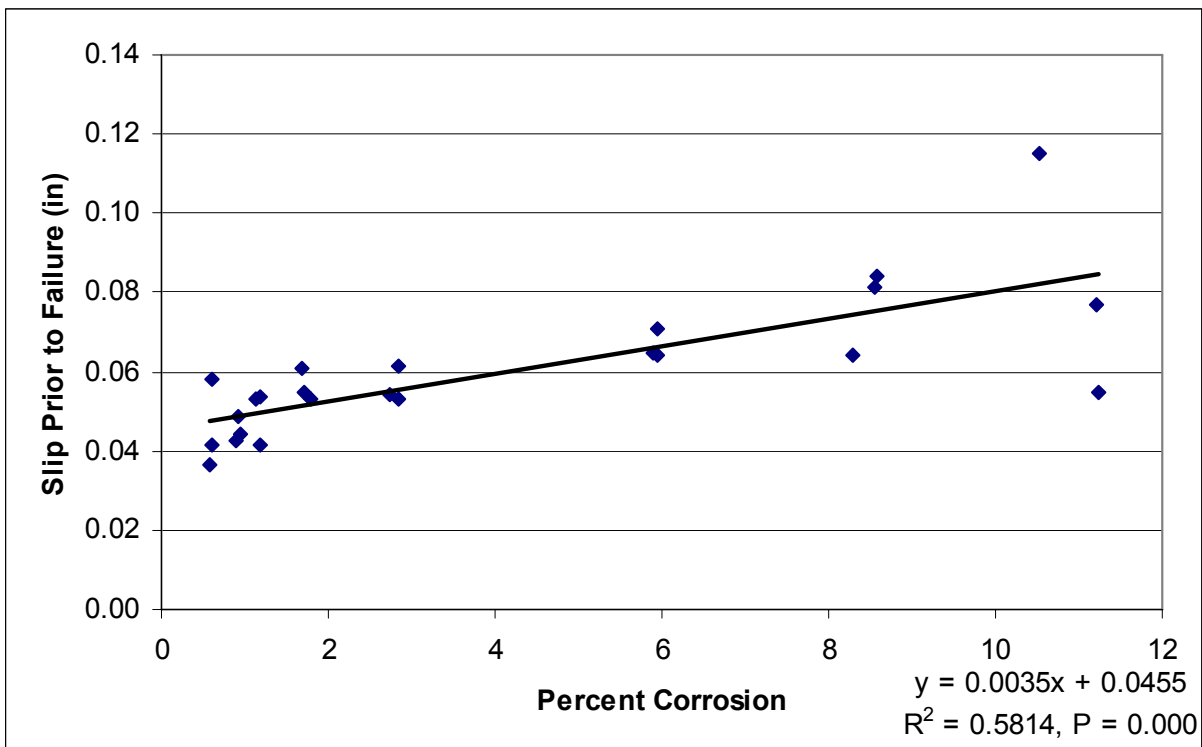


**Figure 4.14 Slip Prior to Failure vs. Percent Corrosion for #5 Rebar Specimens**

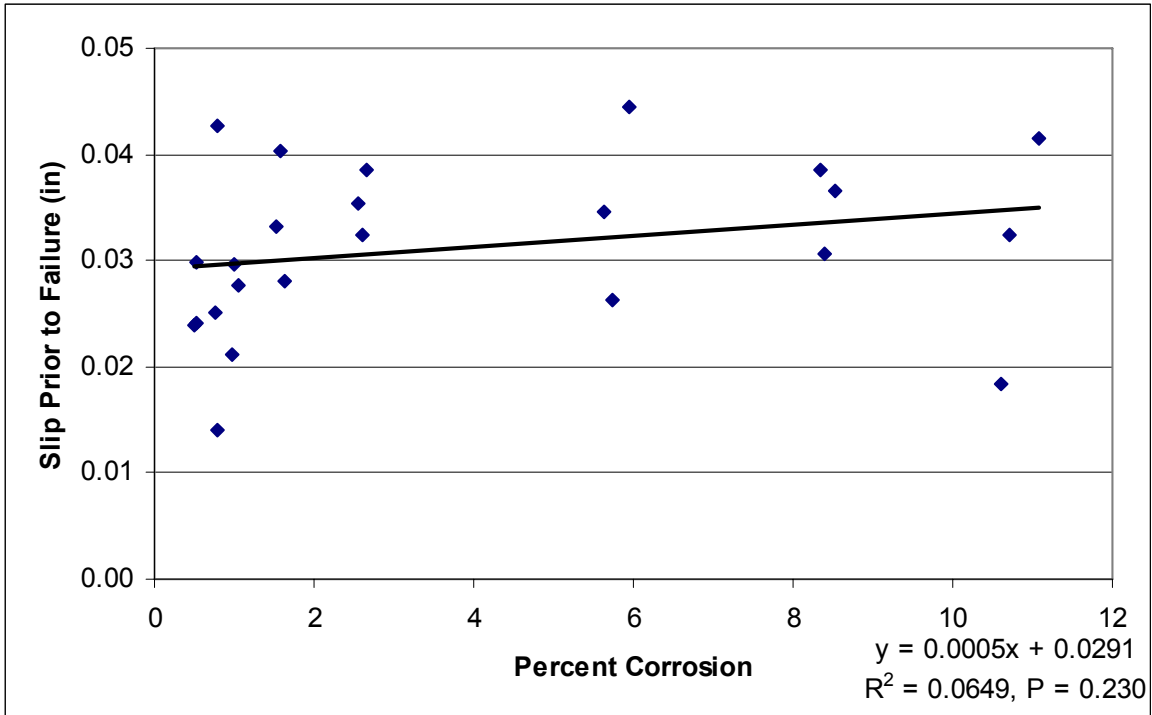


Figure 4.15 Slip Prior to Failure vs. Percent Corrosion for #8 Rebar Specimens

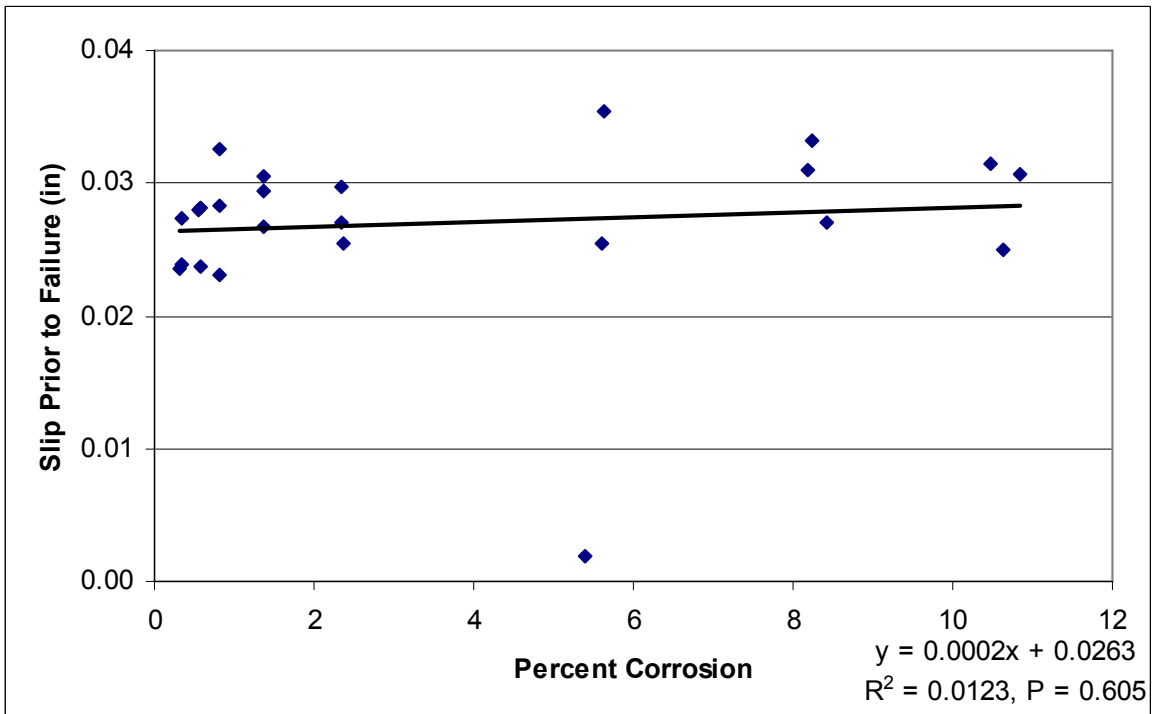


Figure 4.16 Slip Prior to Failure vs. Percent Corrosion for #11 Rebar Specimens

#### **4.4.2 Discussion**

A possible explanation for the observed behavior of the #5 rebar specimens may be the observed relationship between initial slip load and corrosion. With increased corrosion, the rebar, in effect, becomes more “slippery.” Localized crushing of the concrete occurs at a lower load due to reduced projected rib area and increased bearing stress. Bond capacity, however, is maintained as the crushed concrete in front of the ribs bears against intact material along the slip path. The maximum load analysis showed that bond strength was sustained even at higher corrosion. Higher corrosion apparently requires further slippage to engage the crushed concrete and achieve bearing but does not significantly reduce the maximum load.

In addition, study indicates that there is a trend on the slopes of the regression lines. As rebar sizes increase, slopes decrease, and p-values increase. Such a trend implies that corrosion has a lesser influence on slip prior to failure for increasing rebar size. As discussed above, however, the slopes of the populations of the #8 and #11 rebar specimens could be zero (because the sample p-values do not establish statistical significance) and such a trend non-existing. Nonetheless, the potential for such a trend exists.

### **4.5 Maximum Bond Stress**

#### **4.5.1 Results**

Maximum bond stress was an estimated response variable, requiring several assumptions. Maximum bond stress was calculated by dividing the maximum load by an estimated bond area which was based on the nominal dimensions of the rebars. Nominal dimensions of a rebar are equivalent to those of a smooth, round rebar having the same weight per foot as the rebar (MacGregor 1997). For a completely non-corroded rebar, the bond area was estimated as the product of the bond length and the nominal circumference. For a corroded rebar, the nominal circumference was reduced according to the weight of steel loss due to corrosion and sandblasting, assuming a steel density of 490 lbs/ft<sup>3</sup>. A uniform stress distribution was assumed across the estimated bond area for simplicity, although the stress distribution may, in fact, be non-uniform. Table 4.7 lists the maximum bond stress computed for every specimen.

**Table 4.7 Maximum Bond Stress (psi)**

Specimen Name	Maximum Bond Stress	Specimen Name	Maximum Bond Stress	Specimen Name	Maximum Bond Stress
5-0.00-1	3863	8-0.00-1	2193	11-0.00-1	1496
5-0.00-2	4130	8-0.00-2	2274	11-0.00-2	1463
5-0.00-3	4074	8-0.00-3	2249	11-0.00-3	1456
5-0.25-1	4230	8-0.25-1	2034	11-0.25-1	1740
5-0.25-2	4300	8-0.25-2	2416	11-0.25-2	1490
5-0.25-3	3726	8-0.25-3	2165	11-0.25-3	1591
5-0.50-1	4115	8-0.50-1	2623	11-0.50-1	1477
5-0.50-2	3460	8-0.50-2	2214	11-0.50-2	1670
5-0.50-3	4066	8-0.50-3	2064	11-0.50-3	1610
5-1.00-1	3570	8-1.00-1	2629	11-1.00-1	1528
5-1.00-2	2895	8-1.00-2	2239	11-1.00-2	1486
5-1.00-3	3664	8-1.00-3	2036	11-1.00-3	1520
5-2.00-1	4341	8-2.00-1	2472	11-2.00-1	1437
5-2.00-2	4642	8-2.00-2	2234	11-2.00-2	1427
5-2.00-3	4219	8-2.00-3	2418	11-2.00-3	1495
5-5.00-1	4175	8-5.00-1	2074	11-5.00-1	1544
5-5.00-2	3731	8-5.00-2	2365	11-5.00-2	1724
5-5.00-3	4467	8-5.00-3	2541	11-5.00-3	1512
5-7.50-1	4780	8-7.50-1	1972	11-7.50-1	1604
5-7.50-2	4245	8-7.50-2	2207	11-7.50-2	1482
5-7.50-3	3904	8-7.50-3	2631	11-7.50-3	1633
5-10.00-1	4018	8-10.00-1	2235	11-10.00-1	1573
5-10.00-2	3904	8-10.00-2	2416	11-10.00-2	1461
5-10.00-3	3882	8-10.00-3	2467	11-10.00-3	1666

An ANOVA was first performed on the data and results are summarized in Table 4.8. The ANOVA p-values indicate that #5 rebar specimens had at least one set significantly different from the rest, while both #8 and #11 rebar specimens did not.

The Tukey test pairs indicate a significant difference in the maximum bond stress response between 1.0% and 2.0% corrosion and 1.0% and 7.5% corrosion for #5 rebar specimens.

**Table 4.8 Statistical Analysis Results for Maximum Bond Stress**

Bar Size		#5	#8	#11
ANOVA	P-Value	0.037	0.978	0.262
Tukey Test	Pairs	1.0-2.0, 1.0-7.5	n/a	n/a
Linear Regression	P-Value	0.385	0.501	0.382
	R <sup>2</sup>	0.0345	0.0208	0.0349
	Slope	19.744	7.5919	4.4779
	Y-Intercept	3936.1	2268.8	1528.5

Plots of the bivariate linear regression for maximum bond stress versus percent bar corrosion were generated and are shown in Figures 4.17 to 4.19 for #5, #8, and #11 rebar specimens, respectively. The calculated linear regression lines are plotted amongst the data points. Linear regression R<sup>2</sup> values, p-values, and line equations are also included on the figures. The linear regression p-values for all three sets of rebar specimens exceed the 0.05 level of significance, indicating insufficient evidence to reject the null hypothesis. There is therefore insufficient evidence to suggest corrosion has an effect on maximum bond stress.

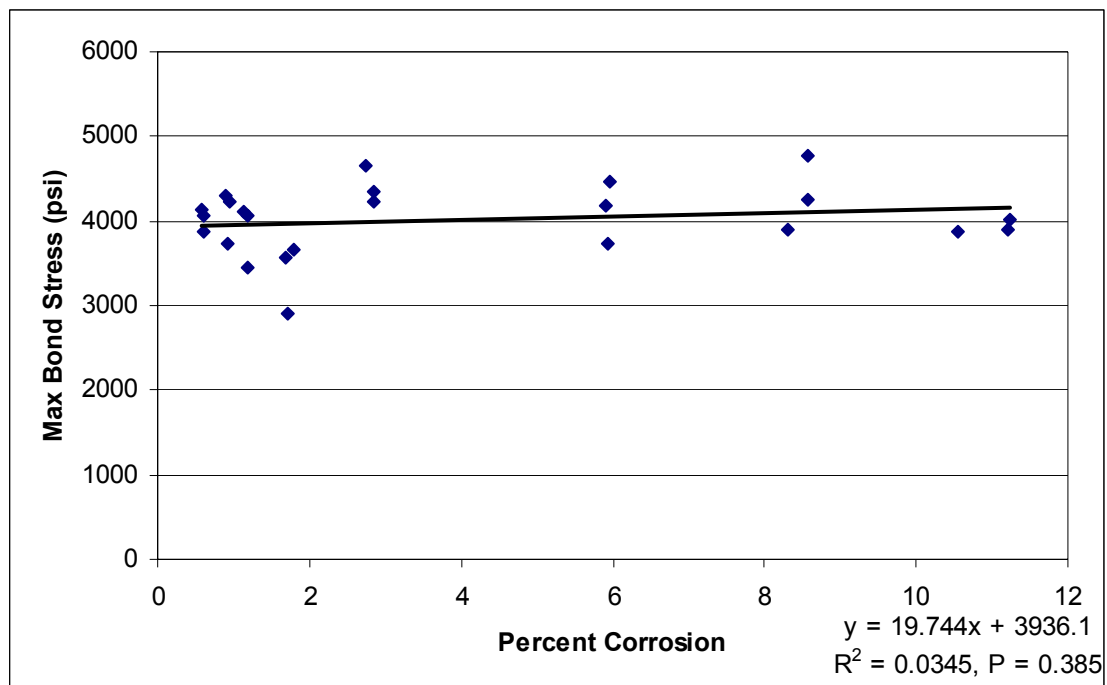


**Figure 4.17 Maximum Bond Stress vs. Percent Corrosion for #5 rebar Specimens**

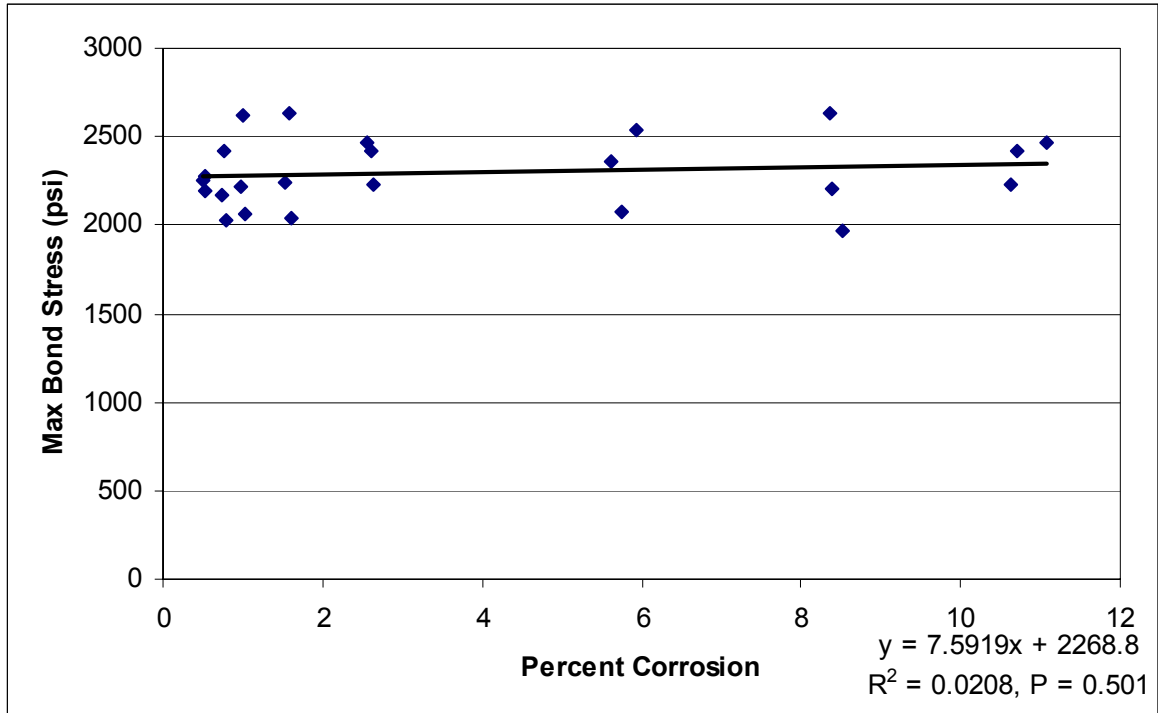


Figure 4.18 Maximum Bond Stress vs. Percent Corrosion for #8 rebar Specimens

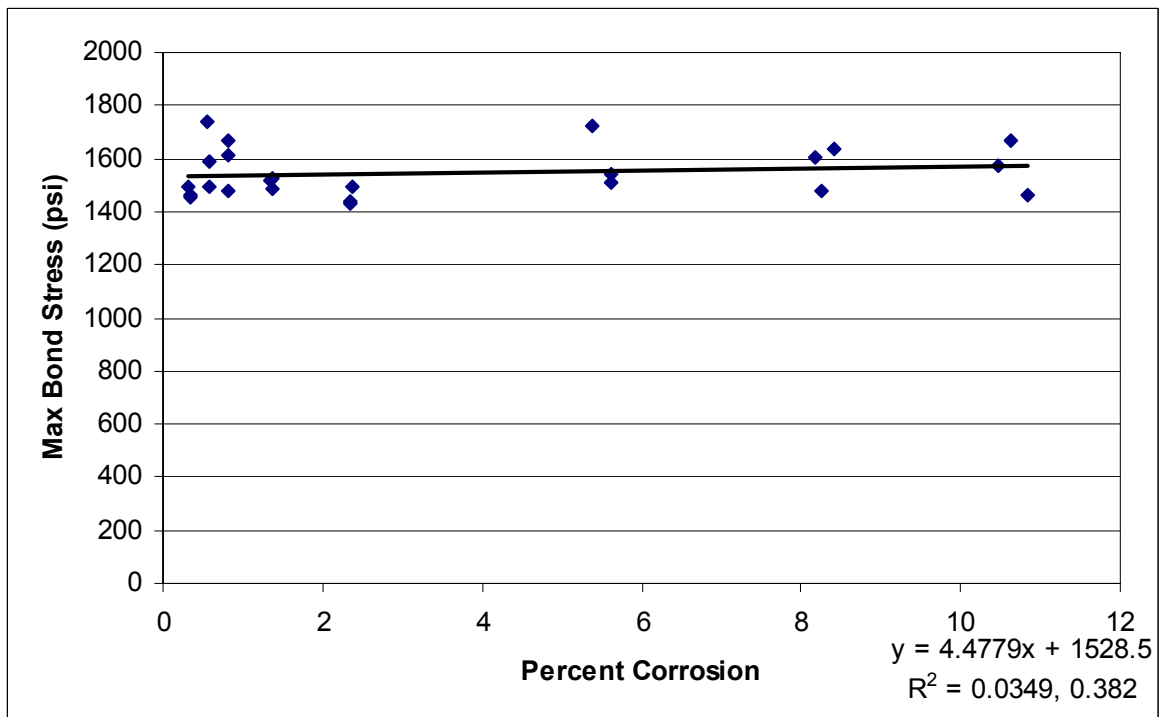


Figure 4.19 Maximum Bond Stress vs. Percent Corrosion for #11 rebar Specimens

#### **4.5.2 Discussion**

Results of statistical analyses are contrary to the initial hypothesis that corrosion would reduce the maximum attainable bond stress. Considering the results of the maximum load analysis and the fact that bond stresses were calculated using the maximum loads, these findings should not be surprising.

Figures 4.17 to 4.19 indicate that maximum bond stresses decrease as bar size increases. The #5 rebar specimens experienced bond stresses substantially higher than either the #8 or #11 rebar specimens. Such a result may imply that concrete strength and concrete cracking may have had an influence on the response variables.

## **5. Conclusions and Recommendations**

### **5.1 Summary**

The study presented in this report evaluated the efficacy of a common repair method for corroded reinforced concrete structural members. The method included encasing in a patch material different size of rebars that had been degraded by corrosion. The objective of the study was to determine the influence of prior to cast rebar corrosion on maximum load, initial slip load, slip prior to failure, and maximum bond stress. The scope of the study included one concrete compressive strength, three rebar sizes, and eight levels of corrosion. A full factorial experimental design was generated utilizing a cantilever beam specimen as the experimental unit. Rebars were corroded prior to casting, sandblasted clean, and cast into the specimens. Pull-out tests were conducted on the rebars, in which applied load and slippage along the bond region were measured. Qualitative and quantitative data were gathered. Response behavior was observed and numerical results were analyzed using several statistical methods and.

### **5.2 CONCLUSIONS**

Conclusions are limited to prior to cast rebar corrosion in the range of 0.00% to 10.0% and concrete with compression strength of 5000 psi.

The first objective was to determine the influence of prior to cast rebar corrosion on the maximum load. There is insufficient statistical evidence to suggest corrosion decreases the maximum attainable load of all sizes of rebar tested.

The second objective was to determine the influence of prior to cast corrosion on the initial slip load. Initial slip load is not applicable to the #5 rebar specimens because all #5 rebar specimens exhibited no distinguishable point of initial slip but rather a more gradual slip. There is insufficient statistical evidence to suggest corrosion decreases the initial slip load of #8 rebars. There is, however, sufficient statistical evidence to suggest corrosion decreases the initial slip load of #11 rebars.

The third objective was to determine the influence of prior to cast corrosion on slip prior to failure. There is sufficient statistical evidence to suggest corrosion increases slip prior to failure for #5 rebars. There is, however, insufficient statistical evidence to suggest corrosion increases slip prior to failure for #8 or #11 rebars.

The fourth objective was to determine the influence of prior to cast corrosion on the maximum bond stress. There is insufficient statistical evidence to suggest corrosion decreases the maximum bond stress of all sizes of rebar tested.

### **5.3 RESEARCH RECOMMENDATIONS**

A revised follow-up study should be conducted to verify the conclusions of this study. Additionally, further research should be conducted to determine the relative rib area of corroded rebars.

A follow-up study would benefit from several modifications. The experimental design should be adjusted for greater statistical “power” which is the ability to correctly reject the null hypothesis when it is, indeed, false (Starmer 2003). Increasing the sample size will increase the statistical power. To do this, first decrease the number of corrosion treatments to three. Low, medium, and high values, such as 0.00%, 10.0% and 20.0%, would be appropriate. The increment between levels of corrosion should be equal. Limit the bar size treatments to one or two. Select rebars no larger than #8 for the sake of practicality in construction and testing. Along with conventional rebars, include smooth rebars to test as a reference. Rebars should be machined to nominal dimensions to match the weight per foot of conventional rebars. The increase in sample size comes by increasing the number of replicates of each treatment. Standard deviations observed in the study presented here will be useful in making that decision.

Selection of a more practical experimental unit would be beneficial. The modified Danish test would be an excellent choice because it is smaller and requires less labor to assemble than the cantilever beam. Also the modified Danish test meets the requirement of keeping the concrete in tension near the bond region. Five gallon buckets would be an ideal form for casting because they are inexpensive, reusable, and require little or no assembly when forming. The application of form oil prior to casting would ensure that they could be stripped from the concrete. Transverse, circular stirrups should be added to provide confinement to the test bar. Longitudinal rebars should also be included to serve as an anchorage for the stirrups and to provide tensile strength to the specimen during pullout testing. Both the rebar to which the rear anchorage is attached and the test rebar should extend well beyond the surface of the specimen to allow space for anchorage and to minimize applied moments that are created during pullout.

The experimental design should particularly address covariates like concrete strength. If possible, the specimens should all be cast in one pour. If that is not possible, then the design should focus on including every treatment in one pour, with replicates obtained in subsequent pours. By so doing, every series of identical treatments will contain concrete from every pour, and concrete strength will no longer confound the results.

Further analysis should also be conducted to determine the relative rib area of corroding rebar. Several approaches could be employed. The most sophisticated, and most costly, would involve performing three-dimensional laser scans on the surface of corroded rebar and generating a digital model of the rebar surface. The model could then be manipulated and studied. Another approach involves performing two-dimensional scans along the length of corroded rebar and calculating the area by counting the number of pixels in the image. Multiple scans should be taken, each time rotating the rebar several degrees about its longitudinal axis. One challenge of such approach would be in obtaining scans that are focused along the edges of the rebar image, where the rebar is raised up above the surface of the scanner due to its curvature. A third method involves cutting thin slices (0.167 in.) of corroded rebar with the thinnest cutting tool available. The slices would then be scanned and the cross-sectional areas calculated by counting pixels. An estimation of the projected rib area and the center-to-center rib spacing could then be estimated based upon the cross-sectional area and thickness of the slices. Additional understanding of the influence of corrosion on relative rib area will help clarify the response behaviors observed in the study presented in this report.

#### **5.4 RECOMMENDATIONS TO UDOT ENGINEERS**

Recommendations are limited to prior to cast rebar corrosion in the range of 0.00% to 10.0%; concrete with compression strength of 5000 psi.; and #5, #8 or #11 rebars. Based on the results of the tests conducted, the following recommendations are made:

- Engineers may simply require that rebars that had been degraded by corrosion be sandblasted clean prior to casting a patching material without compromising the maximum attainable load.

## 6. References

- Almusallam, A., A. Al-Gahtani, A. Aziz, and Rasheeduzzafar. 1996. Effect of Reinforcement Corrosion on Bond Strength. *Construction and Building Materials* 10 (February): 123-29.
- Amleh, L. and S. Mirza. 1999. Corrosion Influence on Bond between Steel and Concrete. *ACI Structural Journal* 96 (May-June): 415-23.
- Auyeung, Y., P. Balaguru, and L. Chung. 2000. Bond Behavior of Corroded Reinforcement Bars. *ACI Materials Journal* 97 (March-April): 214-20.
- Callister, Jr., W. 2000. *Materials Science and Engineering: An Introduction*. 5<sup>th</sup> ed. New York: John Wiley & Sons, Inc.
- Champman, R. and S. Shah. 1987. Early-Age Bond Strength in Reinforced Concrete. *ACI Materials Journal* 84 (November-December): 501-10.
- Corrosion-Club. <http://www.corrosion-club.com/rebarimages.htm>. (Accessed August 2003).
- Darwin, D. and E. Graham. 1993. Effect of Deformation Height and Spacing on Bond Strength of Reinforcing Bars. *ACI Structural Journal* 90 (November-December): 646-57.
- Emmons, P. 1994. *Concrete Repair and Maintenance Illustrated*. 1<sup>st</sup> ed. Kingston, Massachusetts: R. S. Means Company, Inc.
- Fu, X. and D. Chung. 1997. Effect of Corrosion on the Bond between Concrete and Rebar. *Cement and Concrete Research* 27 (December): 1811-15.
- Hamilton, L. 1992. *Regression with Graphics: A Second Course in Applied Statistics*. 1<sup>st</sup> ed. Pacific Grove, California: Brooks/Cole Publishing Company.
- Hawley, W. 1996. *Foundations of Statistics*. 1<sup>st</sup> ed. Orlando: Harcourt Brace & Company.
- Integrated Publishing. [www.tpub.com/doechem1/chem130.htm](http://www.tpub.com/doechem1/chem130.htm). (Accessed August 2003).
- MacGregor, J. 1997. *Reinforced Concrete: Mechanics and Design*. 3<sup>rd</sup> ed. New Jersey: Prentice Hall, Inc.
- Mangat, P. and M. Elgarf. 1999. Bond Characteristics of Corroding Reinforcement in Concrete Beams. *Materials and Structures* 32 (March): 89-97.
- Moore, D. 1995. *The Basic Practice of Statistics*. 1<sup>st</sup> ed. USA: W.H. Freeman & Company.
- Morgan, E. 1998. The Effect of Rust on Reinforcement. *Concrete*. (January): 25-27.
- Rowe, P. Reader in Pharmaceutical Computing. <http://www.staff.livjm.ac.uk/phaprowe/procedures/tukey.htm>. (Accessed August 2003).
- Rutherford, A. 2001. *Introducing ANOVA and ANCOVA: a GLM Approach*. 1<sup>st</sup> ed. Thousand Oaks, California: SAGE Publications.
- Starmer, J. and F. Starmer. MUSC. <http://monitor.admin.musc.edu/~cfs/datamodel/node33.html>. (Accessed August 2003).

Al-Sulaimani, G., M. Kaleemullah, I. Basunbul, and Rasheeduzzafar. 1990. Influence of Corrosion and Cracking on Bond Behavior and Strength of Reinforced Concrete Members. *ACI Structural Journal* 87 (March-April): 220-31.

Vaysburd, A., G. Sabnis, P. Emmons, and J. McDonald. 2001. Interfacial Bond and Surface Preparation in Concrete Repair. *The Indian Concrete Journal* (January): 27-33.